OXYGEN EVOLUTION REACTIONS ON NICKEL, NICKEL OXIDE ELECTRODES USING GALVANOSTATIC METHODS

OXYGEN EVOLUTION REACTIONS ON NICKEL, NICKEL OXIDE ELECTRODES USING GALVANOSTATIC METHODS

by

USMAN GBADEBO AKANO, B.Sc.

A Thesis
Submitted to the School of Graduate Studies
In Partial Fulfilment of the Requirements
for the Degree
Master of Engineering

PART A

McMaster University
1980

MASTER OF ENGINEERING
Department of Engineering Physics

McMASTER UNIVERSITY
Hamilton, Ontario

TITLE: Oxygen Evolution Reactions on Nickel, Nickel Oxide Electrodes using Galvanostatic Methods

AUTHOR: USMAN GBADEBO AKANO, B.Sc. (Ife)

SUPERVISOR: Dr. D.A. Thompson

NUMBER OF PAGES: vi, 67

TABLE OF CONTENTS

ABSTRACT

An electrochemical cell has been designed for use for water electrolysis in 30 w/o KOH solution at 80°C. Various electrode holders and coatings are tested using Ni, NiO as oxygen electrode. A teflon holder in which the electrode press-fits is found to give adequate protection to the electrode.

Epofix resin, when mixed in the ratio of 8 parts epoxy to 1 part hardner, applied to the back face of an electrode, is found to restrict electrode reaction to only the surface of interest. This hardner is stable in 30 w/o KOH solution at 80°C. Current-potential measurements obtained for polished polycrystalline nickel are found consistent with those reported in the literature. The measured electrode potentials on polished nickel are similar to that of electrode which was thermally pre-oxidised in air. This is thought to be due to the fact that the polished nickel surface is rapidly covered with a layer of oxide as soon as oxygen evolution begins.

Dual Tafel regions are observed for each electrode, and the higher slope at the high current densities are thought to be due to oxide formation at these current densities but the absence of hysteresis loops are taken as an indication that the oxide may not be stable with polarisation.

ACKNOWLEDGEMENT

I wish to express my gratitude to Dr. D.A. Thompson, my supervisor, for suggesting this work, for his constant assistance, advice, and tutorage. My gratitude also goes to Dr. W.W. Smeltzer whose ideas are incorporated in the electrochemical cell design and measurements. Sincere thanks also goes to Mark Malloun, Dave Hugson, and John Udak for technical assistance rendered in the course of this investigation. Financial support of the University of Ife and McMaster University is also gratefully appreciated.

LIST OF TABLES

LIST OF FIGURES

CHAPTER 1

INTRODUCTION

Electrochemical energy conversion involves the conversion of the free-energy change (ΔG) of a chemical reaction directly into electrical energy. In electrochemical electricity production using hydrogen and oxygen, the reactants are fed into their respective chambers while the electrolyte (e.g. KOH) is between the two electrodes. Reactions at the anode yield H^+ ions and electrons. The electrons flow to the cathode where O^- ions are formed. The O^- ions flow through the electrolyte to the H^+ and water is formed.

For an ideal fuel cell, the cell terminal potential is constant at the thermodynamical reversible potential value at any value of the current being drawn from it. For a practical cell however, the terminal cell potential decreases with increasing current density. The efficiency of a fuel cell is related to the free-energy change (ΔG) of the chemical reaction taking place, and this in turn to the reversible potential E_γ of the cell. Thus efficiency ε is

$$\varepsilon = \frac{\Delta G}{\Delta H} = - \frac{nFE_\gamma}{\Delta H}$$

where

ΔH = enthalpy change of the reaction.

n = number of electrons transferred from the anode to the cathode during one completion of the overall reaction.

F = Faraday constant.

The main reasons for the decrease in the terminal potential for a practical cell is due to:[1]

(a) the slowness of one or more of the intermediate steps by the reactions occuring at either or both electrodes, i.e. a rate determining step,

(b) slowness of mass transport processes (e.g. reactants and products to or from the electrode),

(c) ohmic losses through the electrolyte; or

(d) ohmic losses at the electrode surfaces.

When all these losses exist, the terminal cell potential becomes

$$E = E_{\gamma} - \eta_{a,a} - \eta_{a,c} - \eta_{con,a} - \eta_{con,c} - \eta_{ohm}$$

where $\eta_{a,a}$, $\eta_{a,c}$ represents the magnitude of the potential losses at the anode and cathode that is due to activation or the rate of reaction at these electrodes.

$\eta_{con,a}$, $\eta_{con,c}$ represent the losses at the two electrodes (anode a, cathode c) that are due to mass transport processes like concentration gradient etc.

η_{ohm} is the magnitude of the potential loss which is attributable to conductivity of the electrolyte. The potentials expressing these losses are termed "overpotentials".

The magnitude of each overpotential increases with current density[2] and hence the terminal potential E decreases. The result is that the efficiency, ε, will decrease for higher current densities.

The objective of this project was to investigate different electrocatalysts introduced into Ni electrodes specifically applied to the oxygen electrode.

Typical value of the cell voltage of an electrolyser is $\sim$ 1.7 to 2.2 V. A reduction in the reversible cell potential is possible by operating at higher temperature, e.g. E_γ = 1.10 V at 150°C compared to 1.18 V at 80°C.[3] This effect is quite small. Thus the efficiency losses are due primarily to the contributions from the activation overpotential losses at the anode and cathode. Typical values for η_a and η_c for water electrolysers having Ni electrodes and operating at 200 mA/cm^2 in 30% KOH at 80°C are 400 and 300 mV respectively.[3] To achieve efficiencies approaching 100% at high current densities ($\sim$1000 mA/cm^2) it is necessary to identify electrocatalysts having higher efficiencies than electrodes presently in use. This project reports a new method of electro-catalyst electrode preparations using ion implantation techniques. Section A details the electrochemical cell design and electrochemical measurements on traditional Ni, NiO anode electrode while section B discusses the introduction of various noble and non-noble catalytic impurities into Ni electrodes and the resulting voltage-current measurements when such electrodes are used as anode in the cell designed in Part A.

CHAPTER 2

ELECTROCHEMISTRY AND ELECTROCHEMICAL CELLS

2.1 Galvanic Cell

Figure 1 shows the diagram of a simple cell, and is useful in defining the terms and concepts common in electrochemistry. The system γ-α-β-β'-α-'γ' represents a closed thermodynamic system.

If

$\alpha \equiv$ anode electrode

then

$\alpha' \equiv$ cathode electrode

$\gamma \equiv$ anode contact (may or may not be the same material as α).

$\gamma' \equiv$ cathode contact (may or may not be the same material as cathode α')

$\alpha/\beta \equiv$ anode-electrolyte interface region.

In operation electrochemical reactions take place in the interface regions α/β and α'/β' between metallic phases and electrolyte. Electrons are transferred across the interfaces from α - γ through the external connection to γ' until they reach the cathode α'. Ion transport from one electrode to the other completes the circuit. Therefore the majority of electrochemical reactions leading to a yield of electrical energy occur at the electrode. The reactions themselves are of various types:

(a) Metal electrode in a solution of its salt. - The reaction at the electrode may be represented as $M^{+} + e^{-} \longrightarrow M$.

(b) Gas Electrodes. - Here the reactant is a gas and the electrode acts only as a donor or acceptor of electrons e.g.

$$\frac{1}{2} H_2 \rightarrow H^+ + e^-$$

The following reactions take place at the interfaces in the case of hydrogen-oxygen cell:[4]

$$\begin{aligned} \frac{1}{2} H_2(\beta) &\rightarrow H^+(\beta) + e^-(\alpha) \\ e^-(\alpha) &\rightarrow e^-(\gamma) \\ e^-(\gamma') &\rightarrow e^-(\alpha') \\ \frac{1}{4} O_2(\beta') + H^+(\beta) + e^-(\alpha') &= \frac{1}{2} H_2O(\beta') \end{aligned} \qquad (1)$$

where the letters in parentheses indicate the phases in which the reactants are located.

(c) Redox Systems. - Here the electrode is an inert conductor and serves as donor or acceptor to one of the oxidation states of some ion in solution e.g.

$$Fe^{3+} + e^- \rightarrow Fe^{2+}$$

For thermodynamic considerations it is assumed that the electrolyte concentration is constant between the two electrodes β and β'.

2.2 Types of Reactions

Like chemical reactions, electrochemical reactions also fall into three main types - single-step, consecutive, and parallel reactions.

Single Step:

In this reaction, the overall reaction is complete in one single step without an intermediate step. An example of this is

$$Li \rightarrow Li^+ + e^-.$$

Consectutive:

This reaction involves two or more steps, one following the other until the final reactants are formed. An example of this is the hydrogen evolution reaction.

Parallel Reaction:

This is not a very common reaction and may be represented as

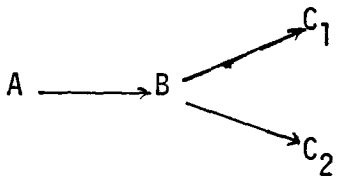

where each step may again involve a number of intermediate single or consecutive steps.

2.3 Concept of a Rate-Determining Step

For an overall reaction involving two or more steps, the velocity of one step is different from that of the other. The step whose velocity determines the velocity of the overall reaction is called the "rate-determining step". The concept holds both for consecutive and parallel reactions. In general the velocity of the overall reaction is approximately equal to that of the rate-determining step, and that the rate-determining step has the highest energy barrier with respect to the initial state of the reaction.

To illustrate this concept one may consider an electric circuit analogy. If a number of resistances R_1, R_2, R_3 connected in series are connected across a battery E, then the current through the circuit is

$$I = \frac{E}{R_1+R_2+R_3} .$$

If R_1 and R_2 are much smaller than R_3 then,

$$I \sim \frac{E}{R_3}$$

which implies that the current flowing through the circuit is almost entirely determined by the single resistance R_3.

Christiansen[5] using the stationary state hypothesis has developed an expression for the velocity of a reaction of the form

$$A_o + A_1 + \ldots + A_n \rightarrow B_1 + B_2 + \ldots + B_n$$

(where the As are the starting materials and the Bs are final products) which proceed through intermediate steps to form first X_1 as an intermediate and B_1 as one final product

$$A_o + A_1 \underset{v_{-1}}{\overset{v_1}{\rightleftharpoons}} X_1 + B_1$$

V_1 is the reaction velocity for the forward reaction and V_{-1} is the reverse velocity. A_2 then combines with intermediate complex X_1 to form B_2 and complex X_2

$$X_1 + A_2 \underset{v_{-2}}{\overset{v_2}{\rightleftharpoons}} X_2 + B_2, \text{ etc.}$$

Considering a specific step g such that

$$v_g \ll v_i \quad \text{for } i = 1,2, \ldots, \quad n \text{ except } i = g.$$

Christiansen showed that

$$v_i \approx v_{-i}$$

i.e. that the forward and reverse reaction velocities are equal for all steps except g, thus showing that all steps except step $i = g$ are all in equilibrium. He also showed that

$$\frac{1}{\vec{v}} \approx \frac{1}{v_g}$$

and

$$\frac{1}{\overleftarrow{v}} \approx \frac{1}{v_{-g}} \tag{2}$$

i.e. the forward and backward velocities of the overall reaction are effectively equal to the corresponding velocities of the g'th step, which is the rate-determining step.

In the case of electrochemical reaction, the velocities of the reactions are expressed in terms of current densities i.

$$\vec{i} = nF\vec{v} \tag{3}$$

where n = number of electrons transferred in the overall reaction

F = Faraday

Eyring[6] and his colleagues have considered the relationship between the activation energy of the overall reaction and the energy of the intermediate states for a reaction which proceeds in the following manner:

$$A \rightarrow B \rightarrow C \rightarrow D \rightarrow E$$

with the step C → D having the highest free energy and B → C the highest activation energy. They showed that the rate-determining step is that with the highest standard free energy of the activated state with respect to the initial state. The overall forward velocity is given by

$$\begin{aligned} \vec{v} &= K_{C\rightarrow D}[C] \\ &= K_{C\rightarrow D}[B] \exp\left(-\frac{\Delta G_{B\rightarrow C}}{RT}\right) \\ &= K_{C\rightarrow D}[A] \exp\left[-\left(\frac{\Delta G_{A\rightarrow B} + \Delta G_{B\rightarrow C}}{RT}\right)\right] \end{aligned} \tag{4}$$

where ΔG represents the difference in standard free energies of the activated complex between C and D, and of the initial state A.

For a chemical reaction of the form

$$A + B \rightleftarrows [AB] \longrightarrow C + D$$

the transition state theory[6] gives the velocity of the reaction as

$$v = \frac{KT}{h}[A][B] \exp\left(-\frac{\Delta G}{RT}\right) \tag{5}$$

where $\Delta G \equiv$ the standard free energy of activation of the reaction. v may be expressed in the form

$$v = \frac{KT}{h}[A][B] \exp\left(-\frac{\Delta H}{RT}\right) \exp\left(\frac{\Delta S}{R}\right)$$

where ΔH is the enthalpy of activation and ΔS is the entropy of activation

Using the above equation, the rate constant of the reaction is

$$K_o = \frac{KT}{h} \exp \frac{\Delta S}{R} \exp(- \frac{\Delta H}{RT}) \tag{6}$$

If the linear dependence of the rate constant on temperature is small (and therefore neglected) then

$$K_o = A \exp(- \frac{E}{RT}) \tag{7}$$

with E now the activation energy of the process. The above equation is the empirical Arrhenius equation.

For a consecutive reaction involving many steps (the rate of which essentially is that of the rate-determining step), the forward and reverse velocities will be[3]

$$\vec{v} = K_g K_1 K_2 \cdots K_{g-1} \frac{[A_o][A_1] \cdots [A_g]}{[B_1][B_2] \cdots [B_{g-1}]}$$

$$= \frac{KT}{h} \frac{[A_o][A_1] \cdots [A_g]}{[B_1][B_2] \cdots [B_{g-1}]} \exp (- \frac{\Delta G_g}{RT}) \tag{8}$$

and

$$\overleftarrow{v} = \frac{KT}{h} \frac{[B_g][B_{g+1}] \cdots [B_{n+1}]}{[A_{g+1}][A_{g+2}] \cdots [A_n]} \exp (- \frac{\Delta G_{-g}}{RT})$$

where K_1 to K_n are the equilibrium constants of the intermediate steps, ΔG_g, ΔG_{-g} are the standard free energies of activation of the forward and reverse directions of the overall reaction.

The efficiencies and power of an electrochemical cell depends on values of rate constants for the charge transfer reactions. These in

turn depend on the velocity of the rate-determining step plus adsorptive properties of reactants and intermolecular forces among the species, but the single dominant factor is the velocity of the rate-determining step.

Rate-determining steps may result from different mechanism controlling the reaction. One may be due to mass transport control[7] (diffusion, diffusion-convection, or ohmic) which also includes the transport of an ion or electron through a solid phase. Homogeneous control refers to situations in which the rate-determining step occurs in solution before the particles reach the electrode and may include chemical reactions in solutions. Rate-determining charge-transfer processes commonly observed in electrode kinetics constitutes Heterogeneous-step control and may also embrace all other kinds of rate-determining surface reactions - nucleation, crystal growth, surface diffusion etc.

An essential feature of electrochemical reaction is that it involves interfacial charge transfer, therefore its reaction rate would be expected (and is indeed found) to depend on the electric potential difference at the interface. The rate constant for an electrochemical reaction may thus be expressed by

$$k = k' \exp(KV)$$

$$= A \exp(-\frac{E}{RT}) \exp(KV) \text{ from eq. (7)} \qquad (9)$$

where V is a metal-solution potential difference and K is a constant.

In practice a symmetry factor β is introduced and it represents the fraction of the contribution of electrical energy to the activation energy of an electron-transfer reaction. Thus

$$k = k_o \exp\ (-\frac{\beta VF}{RT}) \qquad (10)$$

where

k_o = rate constant in the absence of metal-solution potential difference (i.e. $V = 0$)

k = rate constant with $V \neq 0$.

β takes values between zero and one and a frequently used value is $\beta = 1/2$.

2.4 Current-Potential Relations

A very useful term in electochemical kinetics is the current density, i, which is the current per unit area of the electrode surface in Amperes per cm^2. The current density is related to the velocity of reaction through the number of electrons, n, transferred in one complete overall reaction

$$i = nFv$$

Rates of electrochemical reaction are measured in terms of the net current density, where the net current density i is

$$i = \vec{i} - \overleftarrow{i} \tag{11}$$

$\vec{i}$ being the forward current and $\overleftarrow{i}$ the reverse current. By convention a process involving the transfer of electrons from the electrode to the solution is a cathodic reaction while the reverse, a net current flow to the electrode, is an anodic reaction and the associated net current is anodic current.

Steady State Condition

For simple reactions, a steady state is achieved if the time rate of change of the electrode potential, V, at constant current i, or

the time rate of change of the current at constant potential V, is zero i.e. equilibrium condition exists if

$$\frac{dv}{dt} = 0 \text{ at constant } i$$

or

$$\frac{di}{dt} = 0 \text{ at constant } V$$

Thus for a net anodic reaction, the electrode potential is greater than zero, it is equal to zero for a system at equilibrium and is negative for a cathodic process.

The value of the current density for the forward or reverse reaction under conditions of equilibrium is referred to as the exchange current density. The net current density is zero as the reverse and forward currents are equal.

For a redox reaction at electrode A involving only one electron to form a product B

$$A + e^- \rightarrow B$$

the net current density involved, using Eqs. (3) and (10) is

$$i = F[k_f C_A \exp(-\frac{\beta VF}{RT}) - k_\gamma C_B \exp\{(1-\beta)\frac{VF}{RT}\}] \qquad (12)$$

with k_f, k_r the forward and reverse rate constants respectively.
At equilibrium, the current density is the exchange current density and is equal to either of the forward and reverse currents i.e.

$$i_o = Fk_f C_A \exp(-\frac{\beta VF}{RT}) \qquad (13a)$$

$$= Fk_\gamma C_B \exp\{(1-\beta)\frac{VF}{RT}\} \qquad (13a)$$

Here V is the potential difference at equilibrium between the metal electrode and solution. The two equations above can be used to derive an expression for this equilibrium potential

$$V = \frac{RT}{F} \ln \left(\frac{k_f}{k_\gamma}\right) + \frac{RT}{F} \ln \frac{C_A}{C_B} \tag{14}$$

when the concentrations $C_A = C_B = 1$ mole per litre

$$V = V_s = \frac{RT}{F} \left(\frac{k_f}{K_\gamma}\right) \tag{15}$$

where V_s is the standard equilibrium potential.

2.5 Overpotential

The overpotential may be regarded as the extra potential necessary for an electrode so that the rate-determining step of the overall reaction proceeds at the desired rate. In reality it is the potential of the electrode when a net current flows through it minus the equilibrium potential. Thus

$$\eta = V - V_e \tag{16}$$

where

$\eta \equiv$ the overpotential

V = electrode potential with $i \neq 0$

V_e = equilibrium potential

Using Eq. (16) and (13) in (12) we can derive the starting equations for the Tafel equation

$$i = i_o \left[\exp\left(-\frac{\beta\eta F}{RT}\right) - \exp\left\{(1-\beta)\frac{\eta F}{RT}\right\}\right] \tag{17}$$

for a highly cathodic reaction, the overpotential η is highly negative

and the second term in the bracket of (17) is very small. Therefore

$$i = i_o \left[\exp\left(-\frac{\beta n F}{RT}\right)\right]$$

or

$$\ln i = \ln i_o - \frac{\beta n F}{RT}$$

giving

$$\eta = \frac{RT}{\beta F} \log i_o - \frac{RT}{\beta F} \log i \qquad (18)$$

which is equivalent to

$$\eta = a + b \log i,$$

the standard Tafel equation.[8]

A plot of the overpotential η versus log i will give the Tafel parameters a and b

$$a = \frac{RT}{\beta F} \log i_o$$

$$b = -\frac{RT}{\beta F}$$

The Tafel parameter a, is the value of the overpotential at which a net current density of 1 A/cm^2 based on the electrode geometrical area exists. Both a and b have been experimentally found to be constant over several decades of current. The transfer coefficient (= RT/bF) where F is the Faraday (of order unity in present commercial electrolyser) becomes larger with decreasing polarization represented by the Tafel slope b.

For dilute solutions a so-called double layer correction becomes necessary since the assumption of a total potential drop across a compact layer is no longer valid. The potential available at the reaction sites on the compact layer is therefore less than that available to it if no double-layer corrections were made. The result is that the Tafel slope decreases from $-RT/\beta F$ as the potential approaches that of zero charge. For measurements in concentrated solutions, almost all of the potential between the electrode and bulk of the solution is available for reactions at the electrode, and such corrections are not important. Lee,[9] using this fact in his hydrogen evolution measurements confirmed the validity of this approach.

Apart from activation processes controlling an electrode reaction, mass transfer processes may also be involved. Mass transfer processes include diffusion, convection and migration.

Diffusion may arise as a result of differences in the chemical potential of the solute at various points in the solution. Diffusion control usually occurs at high current densities when reactants are consumed faster than they can diffuse from the solution to the electrode, or electrode products being formed faster than they can diffuse away or escape from the electrode surface. This effect is essentially significant for porous electrodes.

Natural convection is due to differences in densities in different parts of the solution resulting from non-uniform temperature or concentration. Variations in concentration are generally due to electrode reactions which consume species near the electrode surface.

Migration is the motion of ions in solution caused by the force exerted on them by the electric potential between cathode and anode during current flow.

2.6 Some Electrochemical Reaction Mechanisms

Knowing the mechanisms of electrochemical reactions is essential for the understanding of electrocatalysis process. Determination of these mechanisms involves five principal steps:[1]

(i) Determination of overall reaction.

(ii) Determination of type of process control - activation or mass transfer control.

(iii) Dependence of surface concentration of reactants on their concentration in solution - Isotherms.

(iv) Nature of adsorbed intermediates and their variation as a function of potential.

(v) Determination by Kinetic parameters e.g. reaction orders, how many electrons are transferred (Stoichiometric number), Tafel slope and exchange current density.

Most reactions of interest on planar electrode surfaces are activation controlled over a wide range of current densities.

2.6.1 Mechanism for Hydrogen Evolution

Many authors have examined the hydrogen evolution mechanism in both acidic and alkaline solutions on various types of electrodes. The net reactions for H_2 oxidation in acid and alkaline electrodes are

$$\frac{1}{2} H_2 \rightarrow H^+ + e^-$$

$$\frac{1}{2} H_2 + OH^- = H_2O + e^- \quad (19)$$

The noble metals and some of their alloys have long been identified as materials that offer sufficient resistance to corrosion in acid media and as being good electrocatalysts at the same time.[4] Knorr and coworkers[10] were the first to conclude that the diffusion of molecular hydrogen is the rate-determining step in the evolution of hydrogen on smooth platinum and palladium electrodes. Later, hydrogen overvoltage on bright nickel electrodes was attributed to a hindrance of the Volmer reaction[11] especially in strong alkaline solutions

$$H_2O + e^- = H_{ad} + OH^- \quad (20)$$

It was suggested that the Volmer reaction above, Eq. (20), is followed by a less hindered Heyrousky reaction:

$$H_2O + H_{ad} + e^- = H_2 + OH^- \quad (21)$$

resulting in the simultaneous oxidation of molecular hydrogen at the Ni electrode. Later it was suggested by Frumkin[12] that reaction (21) is the rate-determining step in the evolution of hydrogen but also that this evolution is limited in part by the Tafel reaction

$$2 H_{ad} = H_2 \quad (22)$$

where H_{ad} is adsorbed hydrogen. The importance of the state of the Ni surface was considered, and it was suggested[13] that the Volmer reactions (20) is rate-determining only on surfaces in an initial state with high

affinity for hydrogen adsorption. In a latter work Bockris et al.[14] carried out simultaneous measurements of current-potential curves and of impedance of the electrode on polycrystalline nickel and on the main faces of nickel single crystals in 4M KOH solution. Their findings indicated that the limiting anodic current was an order of magnitude smaller on nickel electrodes in the steady state. They therefore concluded that the Volmer reaction is the rate-determining step for hydrogen evolution on a surface sparsely covered with H atoms. Hydrogen adsorption was said to occur only at negative values of potential. Lee[9] in a more recent paper studied H evolution from pure Zn, Cd, Fe and Pb electrodes in alkaline solution. He confirmed these findings by concluding that the one-electron transfer step is rate-determining step in the process. Thus it is now generally agreed that of all the three possible rate-determining steps (Eqs. 20-22) in the evolution of hydrogen the Volmer reaction (Eq. 21) is the rate-determining step.

2.6.2 Anodic Evolution of Oxygen

The evolution of oxygen at the anode is a most important reaction in electrolyser research. The reaction is highly irreversible at low exchange current densities on most electrocatalysts.

The paths undergone by the reactants in oxygen evolution are many and varied but generally fall into two broad views.[1] One is that hydrogen peroxide or a peroxide ion is formed as an intermediate in the overall reaction. The other is that the intermediates are principally oxides or hydroxides but that no peroxides are formed. The peroxide intermediate view received greater support when Rozenthal

and others by means of tracer experiments showed that the oxygen evolved electrolytically on PtO surfaces contained the heavy oxygen isotope.

Bockris[14] and others on the basis of experimental observations of Tafel slopes, reaction orders, stoichiometric number and temperature dependence concluded that oxygen adsorption under Langmuir conditions were more probable and that the rate-determining step consistent with their observation is the charge transfer reaction from water to form hydroxyl radicals. Table 1 shows suggested mechanism paths for oxygen evolution. Paths 1, 3, and 4 were those considered by Bockris to be consistent with the constant Tafel slope over large overpotentials observed in their experiment.

In a recent study of oxygen evolution from the surface of platinum oxide electrode in alkaline solution Iwakura et al.[15] observed data which were not satisfied by the previous mechanisms suggested by Bockris and others. They therefore suggested the following steps:

$$S + OH^- = SOH + e^- \qquad \text{step 1}$$

followed by

$$SOH + OH^- = SO^- + H_2O \qquad \text{step 2}$$

(where S stands for a site at the electrode surface) and that the final two steps were those originally proposed by Krasil'shchikov[15a] for nickel electrode in alkaline solution:

$$SO^- = SO + e^- \qquad \text{step 3}$$

$$SO + SO = 2S + O_2 \qquad \text{step 4}$$

It has been pointed out by Appleby[16] in his review that the most probable path for the oxygen electrode on platinum oxide in alkaline solution are the above steps, and that Step 2 is rate-determining at lower overpotentials while Step 1 is rate-determining at higher potentials.

The most generally accepted mechanisms on various electrodes now involve steps such as

$$OH^- = OH_{ads} + e^- \qquad (a)$$

$$OH_{ads} + OH^- = O^-_{ads} + H_2O \qquad (b)$$

$$O^-_{ads} = O_{ads} + e^- \qquad (c)$$

$$O_{ads} + O_{ads} = O_2 \qquad (d)$$

with one of the electron transfer steps[17] rate-determining. Miles[17] did oxygen evolution experiments in alkaline solution on various electrodes (Ni, Rh, Pd, Co, Fe oxides). He found that step [a] is rate-determining for Co and Fe oxides, that step [b] is rate-determining for Ru, Rh, Pd, and Ni oxides and step [c] rate determining for Ir and Pt oxides.

Miles et al.[18] have also observed that for oxygen evolution on Ni electrode in KOH solution at different temperatures, the rate-determining steps also changed with temperature. The slow electron-transfer step being rate-determining at 150°C while the recombination step [d] dominates at 264°C. This change in mechanism they attributed to Neel temperature (TN) for Nickel oxide (TN $\sim$ 250°C).

2.7 Corrosion

The main goal of electrochemistry with respect to electrode development is to achieve those systems in which the rate constants of the electrode are high so that efficiency is maximum. One way to achieve this object is to raise the operating temperature. But at higher temperatures material instability results - the most common form of which is material erosion due to corrosion. Material corrosion is due to electrochemical reactions which cause the surface electrode atoms to ionize. The corrosion of electrodes in cells leads to a decrease in electrode performance with time.

Corrosion may be compared to a cell reaction. Figure 2 shows a cell in which a metal anode M is dissolving into solution:

$$M \longrightarrow M^{+} + e^{-}$$

The released electron reaches the cathode through the external circuit and is subsequently consumed there (resulting maybe in hydrogen evolution or oxygen reduction). If the metal-dissolution reaction has low rate constants, it will be rate determining. Often film formation on the surface results from corrosion.[19] The presence of anions which form complexes with respective electrocatalysts (e.g. Cl^{-} for Pt) enhance corrosion, and must therefore be avoided.

Wagner and Traud[20] assumed the corroding surface as uniform with electron flow homogeneously distributed over the anodic and cathodic surfaces (A_a, A_c). An alternative view is the local cell theory[21] which assumes that the anodic and cathodic reactions during corrosion occur only on certain local sites which will be less than the true area

of the electrode.

The corrosion of nickel in alkaline solutions has been found[22] to be small in alkaline electrolytes at low and medium temperatures. Recent work[22] in 0.2 M KOH indicates that less than 0.1 ppm nickel are dissolved during anodic polarization. Also Ag is known to be insoluble in alkaline solutions at the potentials of interest as the formation of soluble Ag_2O does not occur until much higher potentials.

Various methods are employed to inhibit corrosion including: coating, inhibition by adsorption and both cathodic and anodic protection. In adsorption protection, a corrosion inhibitor is added to the solutions and adsorption of the species on the electrode occurs.

In the anodic protection, the anodic potential is increased until the electrode goes over into a passivating region in which the anodic current becomes very small. The only disadvantage of this method is that not all metals form passive regions, therefore increasing the anode potential will only increase the rate of corrosion. Of course another method will be to use an alloy that is less corrosive in the solution provided its electrochemical properties are adequate.

CHAPTER 3

ELECTROCATALYSIS

The acceleration of the electrodic reaction by a substance which is not consumed in the reaction is electrocatalysis. In general the catalytic substance is the electrode or some material incorporated in it. The electrocatalytic activities of various metals in acid solution for hydrogen evolution have been measured in terms of the exchange current density, i_o. The activity of the metals varies by a factor of 10^9 from Hg to Pt as illustrated by Table 2 taken from Bockris and seems to explain why most investigators invariably use Pt as the hydrogen electrode. Table 3 taken from same source also shows the wide variation in activity for oxygen - dissolution - 10^7 times from Au to Ru.

In some cases the electrocatalyst may also function as a chemical catalyst, interfering with, or aiding the electrocatalysis that may follow. The main objective of electrocatalysis, is therefore to search for materials or their alloys (which may or may not be thermodynamically stable) which have high exchange current densities, i_o for electrode reaction. The overpotential at an electrode is given by the Tafel equation and

$$\eta = \frac{RT}{\alpha F} \ell n \frac{i}{i_o}$$

where i is the current density drawn from the cell and i_0 is the exchange current density as previously defined. An ideal electrode will have a very high exchange current density and therefore the overpotential on its surface will approach zero. A major catalysis problem is the high overpotential at the oxygen electrode. This high overpotential leads to efficiency loss both in voltage and power. One way suggested for reducing the overpotential is to work at higher temperatures, but at higher temperatures corrosion problems also become more important in alkaline solutions. Other approaches require high pressure with the associated increased cost of equipment. Another method to lower the overpotential is to increase the surface area of the electrode (say by surface roughening). This way the electrode particles adsorb reactants from solution and then react electrochemically. The decrease in overpotential resulting from this method will depend on the size of the particle being adsorbed and on the concentration of the catalyst.

A list of work has been done (and is still going on) in the search for suitable electrocatalysts for the oxygen electrode. The types of metal catalysts investigated so far include:

1. Polycrystalline metal powders or bulks.
2. Metals dispersed on polycrystalline oxides.
3. Metals dispersed on clay support.
4. Metals deposited onto organic or carbon matrices.
5. Single crystal metal supports.

Metal ions implanted into polycrystalline Ni, and its oxides for use as oxygen electrode is the subject of Part B of this report.

Many authors have examined ways of lowering both the hydrogen and oxygen overpotentials in alkaline solutions. Lee[23] examined hydrogen overpotentials on pure Zn, Cd, Fe and Pb in 6N KOH solution at 2°, 25° and 50°C and found that the numerical values of the overpotentials are higher (i.e. less negative) at a higher temperature, and in a lower KOH concentration. Miles et al.[24] did a similar study on Ni electrodes at 80°, 150°, 208° and 264°C in 50% (by weight) KOH solution. Their results show that temperature increase has a more striking effect on oxygen evolution reaction than a hydrogen evolution reaction, with each temperature increase producing a lowering of the overpotential. The associated exchanged current density for the oxygen evolution reaction increased by more than three orders of magnitude.

Iwakura et al.[25] reported a highly reproducible overvoltage for oxygen evolution in alakline solutions on platinum oxide (PtO_2) electrode supported by titanium - much more superior than for smooth platinum. In another study by Iwakura[26] on anhydrous RuO_2 electrodes prepared by heating hydrous ruthenium dioxide in air, they reported very good polarization characteristics for the samples heated in air at about 450°C. Further these electrodes were reported to have excellent stability under anodic polarization, and equally important shows little or no anodic dissolution while yielding very low overvoltage for oxygen evolution. Miles et al.[27] examined the effectiveness by various metal oxides under conditions for water electrolysis. Their conclusions about RuO_2 are similar to that of Iwakura[25], but they further found that the effectiveness of various metals for oxygen evolution decreased in the order Ru > Ir $\sim$ Pt $\sim$ Rh $\sim$ Pd $\sim$ Ni $>>$ Co $>>$ Fe.

A striking observation is the higher effectiveness by Ru compared to Ni (a traditional anode material for oxygen evolution), thus ruthenium must be an electrocatalyst to watch in the future.

Lithiation of nickel oxide, having low concentration of nickel cation vacancies compared to pure nickel oxide to produce a more corrosion-resistant electrode was reported by Bacon.[28] Keir and Kutseva[29] also showed that lithium doping increases the rate of oxygen chemisorption, an observation also confirmed by Winter.[30] Nickel oxide, an insulator is generally regarded to exist in a nonstoichiometric form behaving as a p-type semiconductor. Mitoff[31] indicated that cation vacancies exist in the lattice

$$2\ Ni^{2+} + \frac{1}{2}\ O_2 = Ni^{3+} + O^{2-} + h^{\cdot}$$

where h ≡ cation vacancy.

By substitution of monovalent cations like Li+ (or Ag^+) into Ni^{2+} lattices, the p-type conductivity (and Ni^{3+} concentration) will be increased - an observation confirmed by studies of Tseung[32] et al. who also found that at 10 at.% Li_2O, the conductivity of NiO at 25°C increased from 10^{-8} ohm^{-1} cm^{-1} to 1 ohm^{-1} cm^{-1}. In another study on electrochemical reduction of oxygen on lithiated NiO in KOH solution, Tseung[32] also found that the activity increased with increase in Ni^{3+} concentration.

A new method of producing electrocatalysts was reported by Grenness and Thompson.[33] They implanted platinum into substrates of tungsten and tungsten oxide. Their choice of platinum in tungsten was

guided by the fact that the M_1/M_2 (M_1 = mass of platinum, M_2 = mass of tungsten) ratio is ~ 1 thus enhancing a high surface concentration - a beneficial fact since electrocatalytic activity is mainly a surface effect. They found that the electrocatalytic activity of the surface approached that of platinum itself even though a minute amount of platinum had been incorporated. A similar study by Rabette[34] et al. examined the catalytic activity of single crystal supports implanted with platinum ions by ion bombardment techniques. In their preliminary result they found that on annealing the platinum migrates to the surface. Results from catalytic activity measurements are said to be subject of future communications.

With regard to the traditional anode material Ni, improvements have been effected in two ways - development of catalytic semiconducting oxides, and formation of high surface-area nickel catalyst. High surface area nickel can be produced (and has been produced) in several ways - plasma spraying of Ni etc. Another possible way is to bombard the nickel substrate with a high fluence of heavy innert gas e.g. Kr which should lead to formation of cones.

Significant improvement in the conductivity of nickel oxide by lithiation has been reported[29,30,31,32]. The high electrochemical polarization of the nickel electrode at low temperatures is due to the high resistance by the NiO layer to electron transport. References (31,32) document the increase in conductivity of NiO with the Li_2O content. The reaction on the Ni surface is thought to involve the following:

$$\frac{1}{2} O_2 + Li_2O \rightarrow 2Li(Ni)' + 2Ni_{Ni} + 2O_o + 2h$$

where

$Li(Ni)'$ ≡ Li occupying nickel sites

Ni_{Ni} ≡ Ni on nickel sites

h ≡ holes

O_o ≡ oxygen on oxygen sites

A similar mechanism can be assumed to take place in the case of Ag incorporated in Ni

$$\frac{1}{2} O_2 + AgO \rightarrow Ag(Ni)' + Ni_{Ni} + 2O_o + h$$

CHAPTER 4

EXPERIMENTAL

4.1 Cell Design

The electrochemical cell consists of a 3-compartment cell made of Teflon and is shown in Fig. 3. The main cell (teflon beaker) contains the electrolyte and is provided with a cover to minimize contamination problems that may be due to the environmental or reflux action. The second compartment, immersed in the electrolyte and resting on the cover of the main cell contains the reference electrode (labelled 4 in Fig. 3a) while the third, similarly situated in the main cell, contains platinum counter electrode (1) for the working electrode (Ni, NiO, implanted Ni, etc.). The reference electrode compartment was provided with a 2 mm diameter Luggin capillary (L) to ensure fresh electrolyte is always available in the reference compartment. A high surface area counter electrode for the reference cell was made from platinum gauze tightly wound to a platinum lead. The third compartment containing the counter electrode for the working electrode also has a 1/4" hole drilled at the bottom. The working electrode is held flush in a teflon holder and baths in the solution while facing the luggin cappilary. Appropriate holes were provided on the cell cover so that electrical connections could be made to the electrodes. Evolved hydrogen in the reference compartment leaks away through a rubber tubing, one end of which was attached to cover the mouth of the reference cell, while the other dipped in a flask containing water. The reference electrode used in this experiment is

that described by Giner.[35]

The electrode holder is shown in Fig.3b. It consists of a solid teflon with a 4 mm diameter hole drilled through ∿80% of its length. A ∿1/2" diameter groove was made on one face of the teflon. A 30 thousandth of an inch hole was then drilled at ∿45° to link with the first hole. The electrical connection to the electrode was passed through this hole and external connection made through the larger hole. With a little amount of pressure applied, the sample sits firmly in the groove and flush with the teflon edge. The back of the electrode, its electrical lead and the leads of the other electrodes in the solution were covered with epoxy. The special electrode holder ensured that no electrolyte got to the back face of the electrode and the epoxy also gave double protection while ensuring that no reaction took place at the back of the electrode or on the electrical leads. The epoxy coating was made from 8 parts epoxy and 1 part hardener. Figure 4 shows the photo of the cell assembly and the individual cells with the electrodes.

The solution was made from 180 gm "baker Analyzed" (99.95% purity) KOH and 420 mls of doubly-distilled water (making 30% by weight KOH solution).

The cell was placed in an oil bath and heated by an oil-immersion heater electrically. The temperature was controllable to ± 1/2°C. The heating oil was stirred continuously. The oil was heated until the electrolyte temperature attained 80°C, and then was maintained there for at least 30 minutes before measurements began.

Each nickel electrode was mechanically polished using various grades of emery paper. Before polishing starts each electrode was cut into ∿ 9 mm diameter discs from rolled nickel ingots annealed in argon atmosphere. Mechanical polishing on emery paper was followed by polishing on rotating wheel using 6, and then 1 micron diamond paste. Some of the samples were examined as polished while some had ∿ 400 Å of oxide thermally grown in air according to the method of Graham and Cohen.[36]

To measure the activity of the oxygen electrode, a constant current of 1 mA was passed between the platinum counter electrode and the Dynamic Hydrogen Electrode (DHE). A current sweep from 0.1 mA up to 1A was passed through the working Ni (or NiO) electrode and its Pt counter electrode. Starting at a current of 100 mA the current was reduced in steps from 100-80-60-50-30-20-10-1-0.1 mA taking ∿ 2 minutes to move from one current value to the next. The current was then swept up 0.1-1-10-20-30-40-50-60-80-100 mA making one complete sweep. At each current value both the overpotential η on the Pt hydrogen electrode Vs. DHE reference electrode as well as the total cell potential vs. DHE reference electrode were measured. The sweep was then repeated until ∿ 8 complete sweeps have been made. Then the current was taken up in steps to 1A (100-200-400-600-800-1000 mA). The system was then left to stabilize at this current value for about 30 minutes. We then undertook a down sweep: 1000-800-600-400-200-100-50-20-10-0.1 A and then an upward sweep. Six such sweeps were undertaken for each day. At the end of the first day current-potential measurements, the cell was left running at a reference current of 1 mA and

counter-working electrode current of 100 mA for ∿ 18 hours, when the 2nd day measurements - a repeat of the previous day's procedure - were carried out. Before beginning the measurements, the DHE reference electrode was usually depolarized by raising its current to ∿ 25 mA (instead of the usual 1 mA).

Figure 3(c) shows a schematic of the electric circuit used in this experiment. A is a stabilized current source with a very high input impedance ∿20,000 ohms and can supply a well stabilized current from 0-25 mA. This source was used to polarise the reference cell. A current of 1 mA taken from this source is passed through Pt gauze counter electrode and the DHE. B is an hp 6186B DC current source having a high internal impedance ∿40,000 ohms and is capable of delivering from 0.1 to 100 mA. Low current density polarisation of the working electrode was carried out using this current source. For higher current density polarisations (200-1,500) we employed a Heat Kit Regulated Low Voltage power supply (C in the Figure) with high internal impedance. The electrode potentials were measured using type 3800 A Digital Multimeter. During measurements both the cell potential and the overpotential of the reference electrode were recorded using a Rikadenki (RDK) chart recorder and no formal measurements are begun until these potentials are observed steady.

CHAPTER 5

RESULTS AND DISCUSSION

Several attempts were made to restrict reaction at the Ni electrode to only one face of the electrode. As a result a number of electrode holders were designed and tested. The first sample had polymethane applied to its back face, the second had its back coated with parafin wax while the third had 5-minute epoxy. The parafin wax was cleaned off the backing in $\sim$ 1 hour while the 5 minute epoxy separated out into solution as well indicating the instability of these protectives in 30% by weight KOH at 80°C. Figures 5-7 show the current-potential relationships for these electrodes respectively. Potential drop due to IR losses were not corrected for, (nor were corrections for overpotential made) and the potentials were measured vs. DHE. The fact that the potentials are relatively low compared to reported data is an indication that the backings were not effective in preventing oxygen evolution reaction at the back surface of the sample. Figure 8 compares these results with that reported by Miles[24] et al. for current sweeps between 0.1 mA and 100 mA. Figure 9 compares our results for the same 3 electrodes with that reported by Lu and Srinivasan (their data is for H_2 evolution and potentials were measured vs. reversible electrode) in 8 N KOH at 23° and 90°C; and also with that of Miles. Further effort to prevent oxygen evolution from the back surface led to holding the electrode in a teflon holder. The first test electrode (called Ni(4)) was just pressed-fit into the holder - no epoxy backing.

The second Ni(5) had epoxy backing plus teflon tape around the holder threads. Ni(6) and Ni(7) were tested with a new holder with bigger threads. Ni(6) had teflon tape behind it and around the threads, while Ni(7) had tape around the threads, epoxy on electrode Pt lead, threads and behind the sample. It was observed that somehow KOH solution still managed to get to the back of the sample and presumably oxygen evolution reaction occured there. These were borne out by the lower cell potentials recorded (as shown in Fig. 10). But obviously there is an improvement over the previous measurements.

A new electrode holder without threads and with hole as little as 30 thou' for the electrode contact was constructed. The current-potential measurements for the first electrode tested with this holder is also shown in Fig. 10 (Ni(8)). The two curves represent the measurements for the first and second days. The curve shows a close agreement with the work of Miles.[24] Also the good agreement between the curve obtained on the first day and that of the second day is also remarkable indicating good electrode stability over the period. Two distinct Tafel regions (≡ two different slopes) are also apparent - one at low current densities and the other at higher current densities. The measured electrode over-potential throughout the experiment was ∿ 40-45 mV, a value in good agreement with that measured by Miles et al. (45 mV) at 80°C in 30 w/o KOH.

The above discussions have concerned polarization characteristics when the polarizing current was no higher than 100 mA. Figure 11 shows the current-potential (vs. DHE) characteristics when the current sweep was between 0.1 mA and >1.0 A. The main feature is the rapid increase in potential when the current density exceeds ∿ 100 mA/cm^2. This effect

has been well documented[37] and is believed to be due to the rapid growth of NiO at these current densities. Since NiO is known to be only semi-conducting and has a high resistance to electron transport, one can then see the reason for the high electrochemical polarization on the Ni surface. A new approach to lower this rapid increase in electro-chemical potential is the subject of Part B of this report. A value of 0.068 for the Tafel slope obtained with Ni(8) per decade at low current densities compares well with that obtained by Miles and Huang[27] (b = 0.071/decade) and that of Miles and Lu[24] in 50 w/o KOH at 80°C (0.095 V/decade).

Figure 12 shows the current-potential relations obtained for oxygen evolution on the surface of nickel electrode on which $\sim$ 400 Å of oxide has been grown in air. Polished Ni electrodes were put in an oven at atmosphere at 450°C for 20 minutes. At this temperature and time of exposure $\sim$ 400 A oxide should result on the surface.[36] One immediate observation from Fig. 12 is the relatively large difference between the curve for the first day and that for the second day (at least compared with polished Ni) in the 0.1-100 mA/cm^2 current density range. There is a better degree of reproducibility at the higher current densities as evidenced by figures 13 and 14.

Microscopic examination of the electrode surface after the current potential measurements show that the polished Ni surface is more subject to anodic disolution, whereas little or no corrosion products were present on the Ni electrode thermally oxidized in air before electrochemical measurements.

Figure 15 shows the curve of overpotential versus current density obtained on Ni and NiO electrodes for galvanostatic sweeps between 0.1 to ∿150 mA/cm^2 while figure 16 shows similar measurements for high current density sweeps (0.1 - ∿1,500 mA/cm^2). The curve for the polished nickel is similar to that obtained by Miles[24] in 50 w/o KOH solution at 80°C. Both at the medium and high current densities there is not much difference in the overpotentials measured on the polished and oxidised electrodes. This is probably not surprising since the polished electrode will be rapidly covered with an oxide as soon oxygen evolution begins during the experiment.

Tables 4 and 5 show the kinetic parameters for oxygen evolution on these electrodes calculated from figures 15 and 16. The Tafel slopes obtained at low overpotentials (0.064 for polished Ni, and 0.07 for NiO electrode) are compared to that obtained by Miles[24] (b = 0.095) in 50 w/o KOH at the same temperature (80°C). The obtained transfer coefficients (α = 1.098 on polished Ni, 1.0 on NiO) are consistent with an electron transfer step being rate-determining[24] in oxygen evolution at these overpotentials. No exchange current densities were estimated at the lower current densities but high exchange current densities were obtained for electrode polarisations from 0.1 to ∿150 mA/cm^2 (i_o ∿ 3 x 10^{-4} A/cm^2), and 0.1-1,500 mA/cm^2 (i_o ∿4 x 10^{-1} A/cm^2) indicating that at these current densities, the electrode process is less irreversible.

CHAPTER 6

CONCLUSIONS

1. The Epofix resin when mixed in the ratio epoxy: hardner of 8:1 and let set for ∿10 hours is quite stable in 30 w/o KOH solution at 80°C and gives an effective protection to the back surface of the electrode.
2. The kinetic parameters obtained on Ni and NiO electrodes are comparable to those reported in the literature under similar conditions.
3. Dual Tafel regions were observed at higher current densities. This change may be due to a change in mechanism for oxygen evolution, or due to an oxide formation on the electrode surface, or another step other than electron transfer step being rate-determining.
4. A better electrode stability with time was observed with polished Ni electrode compared to a nickel electrode pre-oxidised thermally in air.

REFERENCES

1. Bockris and Srinivasan, "Fuel Cells: Their Electrochemistry", McGraw-Hill, 1969, p. 20.

2. Bockris and Srihivasan, "Fuel Cells: Their Electrochemistry", McGraw-Hill, pg. 22, 1969.

3. Martin Harmeli, AECL, Chalk River, Private Communication.

4. M.W. Breiter, "Electrochemical Processes in Fuel Cells", Springer-Verlag, New York, 1969, p. 6.

5. Christiansen, J., Physik. Chem. Let. B., 33, 145, (1946).

5a. Bockris and Srinavasan, "Fuel Cells: Their Electrochemistry", McGraw-Hill, 1969, p. 59.

6. Alasstone, S., Laidler, K.J. and Eyring, H., "The Theory of Rate Processes", McGraw-Hill Book Co., New York, 1941.

7. Bockris, J., J. Elelectrochem. Soc., 98, 153c (1951).

8. Tafel, J., Physik Chem., 50, 641 (1905).

9. Lee, T.S., J. of Electrochem. Soc. Vol. 118, No8 (1971) 1278-1282

10. Kandler, L., Knorr, C.A. and Schwitzer, Z. Physik. Chem. A 180, 281 (1937).

11. Levina, S., Frumkin, A.: Acta Physicochem. U.S.S.R. 11, 21 (1939).

12. Frumkin, A., Discussion Faraday Soc. I, 57 (1947).

13. Makrides, A.C., J. Electrochem. Soc. 109, 977 (1962).

14. Bockris, J.O.M., J. Chem. Phys. 24, 817, (1956).

15a. Krasilshchikow, A.I., J. Phys. Chem. (USSR), 27, 512 (1953).

15. Iwakura, C., Fukuda, K. and Tamura H., "Electrochimica Acta. (1976), Vol. 21, pg. 505.

16. Appleby, A.J., Catalysis Reviews, 4, 211 (1970).

17. Miles, M.H., Huang, Y.H., J. Electrochem. Soc., Vol. 125, No. 12,(Dec. 1978.) 1931

18. Miles, M.H., Kissel, G., Lu, P.W., Srinivasan, S., J. Electrochem. Soc., Vol. 123, No. 3,(March 1976.) pp. 332-336

19. Bockris, J. and Srinivasan, S., "Fuel Cells - Their Electrochemistry", McGraw-Hill, New York, (1969) pp. 115

20. Wagner, C. and Traud, W., Z. Electrochem. 44, 391 (1938).

21. Uhlig, H., "Corrosion Handbook", John Wiley & Sons Inc., New York. (1948)

22. Breiter, M.W., "Electrochemical Processes in Fuel Cells", Springer-Verlag, New York, 1969, pg. 214.

23. Lee, T.S., J. Electrochem. Soc., Vol. 118, No. 8, (Aug. 1971) pp 28.

24. Miles, M.H., Kissel, G., Lu, P.W., Srinivasan, S., J. of Electrochem. Soc., Vol. 123, No. 3, pg. 332. (March 1976).

25. Iwakura, C., Fukuda, K., Tamura, H., Electrochemica Acta, Vol. 21. (1976) 501

26. Iwakura, Chiaki, Kazuhiro Hirao and Hideo Tamura, Electrochemica Acta Vol. 22, pg. 335. (1977)

27. Miles, M.H., Huang, Y.H., J. Electrochem. Soc. Vol. 125, No. 12, (Dec. 1978) 1931

28. Adams, A., Bacon, F., and Watson, R.G.H. in Fuel Cells ed. Mitchel, Jr., p. 129, Academy Press, London, 1963.

29. Keir Kuseva, Bull. Acad. Sci., USSR Chem. Div. 5, 775 (1955).

30. Winfer, E.R.S., J. Catal. 6, 35 (1966).

31. Mitoff, S.P., J. Chem. Phys., 35, 887 (1961).

32. Tseung, A.C.C., Hobbs, B.S. and Tantram, A.D.S., Electrochimica Acta, 1970, Vol. 15. pg. 473-481

32a. Tseung, A.C.C., Bevan, H.L., J. of Material Science 5 (1970), p. 604-610.

33. Grenness, M., Thompson, W.W., J. Applied Electrochemistry 4 (1974), p. 211-218.

34. Rabette, P., Deane, A.M., Tench, A.J., Che, M., Chemical Physics Letters, Vol. 60, No. 2. (1979) 348.

35. Giner, J., J. Electrochem. Soc. 111, 376 (1964).

36. Graham, M.J., Cohen, M., J. Electrochemical Soc., July 1972, Vol. 119, No. 7, Pg. 879-883.

37. **M.H. Miles, E.A. Klaus, B.P. Gunn, Locker, W.E. Serafin and S. Sirinivasan: Electrochimica Acta (1078) vol. 23, pp 521-526.**

Table 1: Tafel slopes for the most probable mechanism in the oxygen-electrode reaction.*

Reaction Path	Tafel Slope (anodic) low η	high η
1. "Oxide" Path:		
$4M + 4H_2O \rightarrow 4MOH^- + 4H^+ + 4e^-$	$\frac{2RT}{F}$	
$2MOH \rightarrow MO + MH_2O$	RT/2F	
$2MO \rightarrow O_2 + 2M$	RT/4F	
2. "Electrochemical Oxide" Path		
$2M \rightarrow H_2O \rightarrow 2MOH + 2H^+ + 2e^-$	2RT/F	
$2MOH + 2M + H_2O \rightarrow 2MO + 2MH_2O + 2H^+ + 2e^-$	2RT/3F	2RT/F
$2MO \rightarrow O_2 + 2M$	RT/4F	
3. "Hydrogen Peroxide" Path		
$4M + 4H_2O \rightarrow 4MOH + 4H^+ + 4e^-$	2RT/F	
$2MOH \rightarrow MH_2O_2 + M$	RT/2F	
$MH_2O_2 + MOH \rightarrow MOH_2 + MO_2H$	RT/3F	
$MO_2H + MOH \rightarrow MH_2O + M + O_2$	RT/3F	
4. "Metal Peroxide" Path		
$4M + 4H_2O \rightarrow 4MOH + 4H + 4e^-$	2RT/F	
$2MOH \rightarrow 2MO + 2MH_2O$	RT/2F	
$MO + MOH \rightarrow M + MHO_2$	RT/3F	
$MHO_2 + MOH \rightarrow O_2 + M + MH_2O$	RT/4F	

continued...

Table 1 (continued)

Reaction Path	Tafel Slope (anodic) low η [1]	high η
5. "Alkaline" Path of Hoar		
$2M + 2H_2O \rightarrow 2MOH + 2H^+ + 2e^-$	2RT/F	
$2MOH + 2H_2O \rightarrow 2MH_2O_2^- + 2H^+$	RT/F	
$2MH_2O_2^- \rightarrow M + MO_2^{2-} + H_2O$	RT/2F	RT/F
$MO_2^{2-} \rightarrow M + O_2 + 2e^-$	RT/3F	
6. Path of Krasilshikow:		
$2M + 2H_2O \rightarrow 2MOH + 2H^+ + 2e^-$	2RT/F	
$2MOH \rightarrow 2MO^- + 2H^+$		
$2MO^- \rightarrow 2MO + 2e^-$	2RT/3F	2RT/F
$2MO \rightarrow O_2 + 2M$	RT/4F	

*from: Damjanovic, A., Dey, A., Bockris, J. Electrochem. Acta., 11, 791 (1966).

TABLE 2

Exchange current densities for the hydrogen electrode reaction on some metals.*

Metal	Normality of H_2SO_4 Electrode	i_o amps/cm^2 at 25°C
Pt	0.5	1×10^{-3}
Rh	0.5	6×10^{-4}
Ir	1.0	2×10^{-4}
Pd	1.0	1×10^{-4}
Au	2.0	4×10^{-6}
Ni	0.5	6×10^{-6}
Nb	1.0	4×10^{-7}
W	0.5	3×10^{-7}
Cd	0.5	2×10^{-11}
Mn	0.1	1×10^{-11}
Pb	0.5	5×10^{-12}
Hg	0.25	8×10^{-13}
Ti	2.0	6×10^{-9}

*Taken from Bockris and Srinivasan: "Fuel Cells: Their Electrochemistry".

TABLE 3

Exchange current densities for the oxygen electrode reaction on some metals at 25°C.*

Metal	i_o in 0.1 N NaOH (amp/cm^2)
Pt	1×10^{-10}
Pd	1×10^{-11}
Rh	3×10^{-13}
Ir	3×10^{-14}
Au	4×10^{-15}
Ag	4×10^{-10}
Ru	1×10^{-8}
Ni	5×10^{-10}
Fe	6×10^{-11}
Cu	1×10^{-8}
Re	4×10^{-10}

* Taken from "Fuel Cells: Their Electrochemistry" by Bockris, J. and Srinivasan, S.

Table 4: Kinetic parameters on oxygen electrodes for 0.1-150 mA/cm^2 galvanostatic polarisation.

Electrode	Tavel Slope, b(V)			Exchange current density	Transfer Coefficient
	low η	high η	Rev[12]*	i_o A/cm^2 high η	α
Polished Ni	0.064	0.31	0.095	2×10^{-3}	1.098 0.227
Ni with Thermally grown oxide	0.07	0.32	—	3×10^{-3}	1.0 0.226

*Tafel slope measured by Miles[12] for oxygen evolution on polished Ni in 50 w/o KOH.

Table 5: Kinetic parameters on oxygen electrodes for 0.1-1500 mA/cm^2 galvanostatic polarization.

Electrode	Tafel Slope, b(V)		Exchange Current Density	Transfer Coefficient
	low η	high η	i_0 A/cm^2 high η	α
Polished Ni	0.064	—	4×10^{-1}	1.10
NiO	0.07	—	4×10^{-1}	1.00

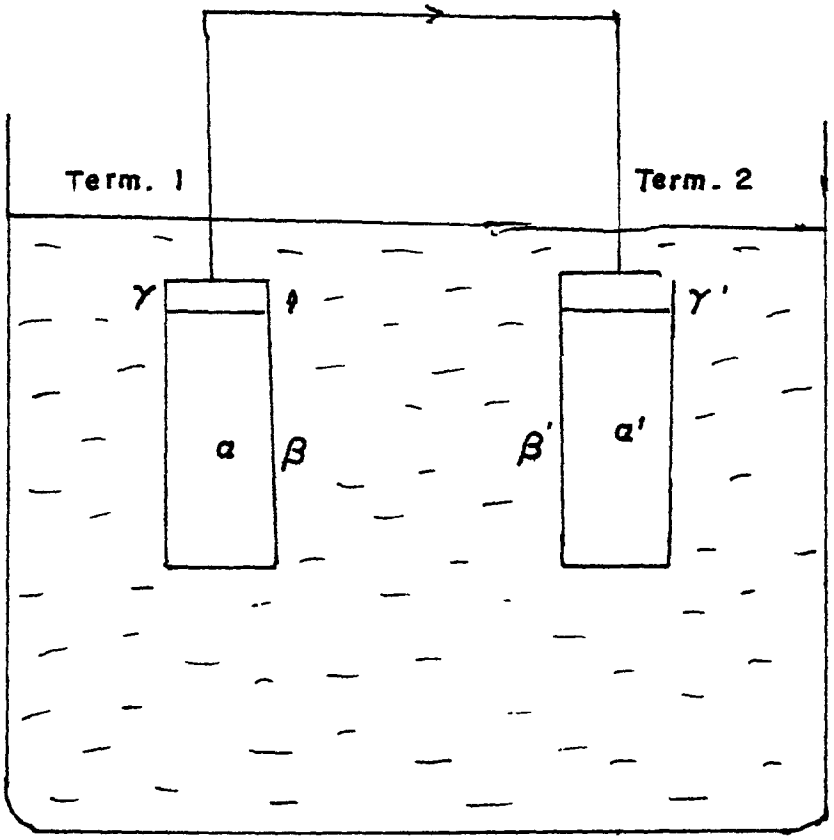

α, α' —— electrodes

β, β' —— solid-liquid interface

γ, γ' —— electric contacts

Figure 1: Schematic of a galvanic cell.

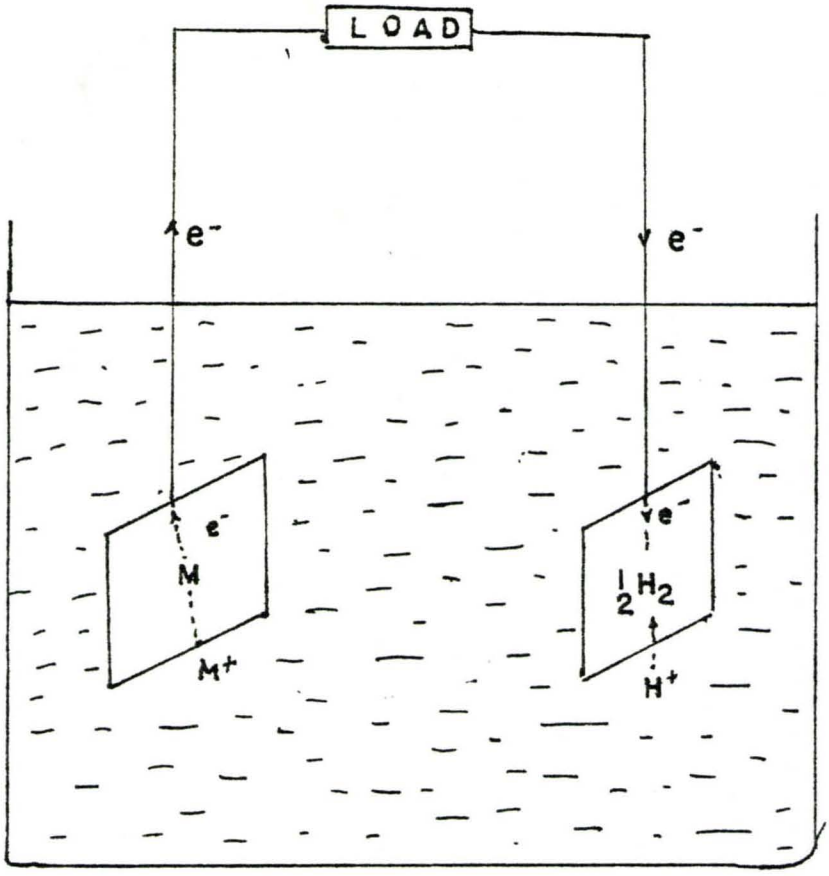

Figure 2: Illustration of corrosion to cell reaction.

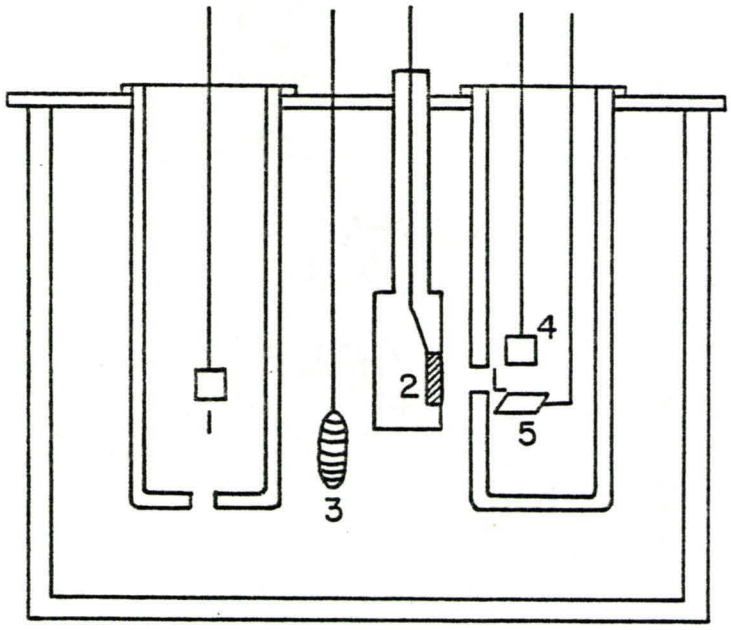

Figure 3(a): The 3-compartment cell.

1 = Pt counter electrode.

2 = Ni oxygen electrode.

3 = Pt gauze which serves as the counter electrode for the reference compartment.

4 = Platinized Pt (Pt black) reference electrode.

L = Luggin carpillary.

5 = Dynamic Hydrogen Electrode.

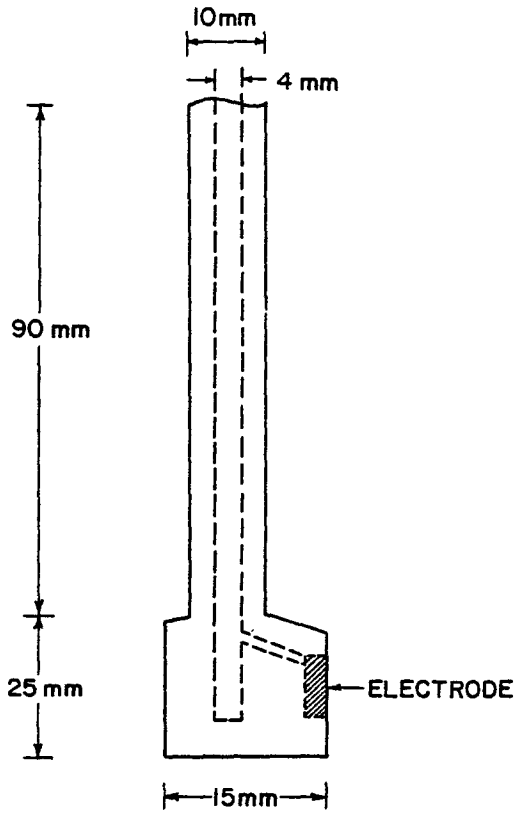

Figure 3(b): Teflon Electrode holder.

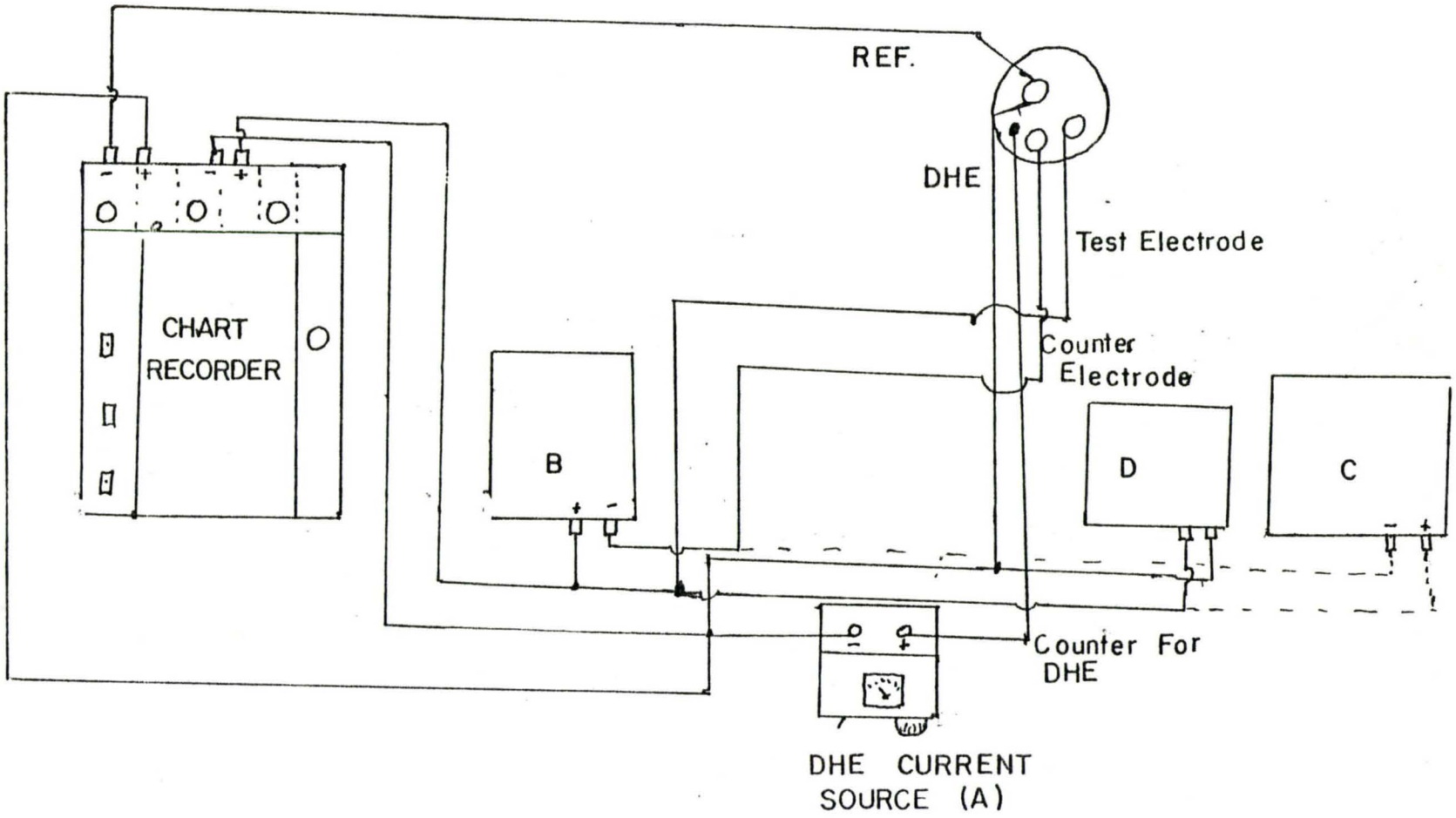

B,(C) ≡ Current source for working electrode.

D ≡ Digital voltmeter for measuring electrode potential.

Figure 3(c): Schematic of the electric circuit employed.

A ; CELL ASSEMBLY

B ; ELECTRODE HOLDER

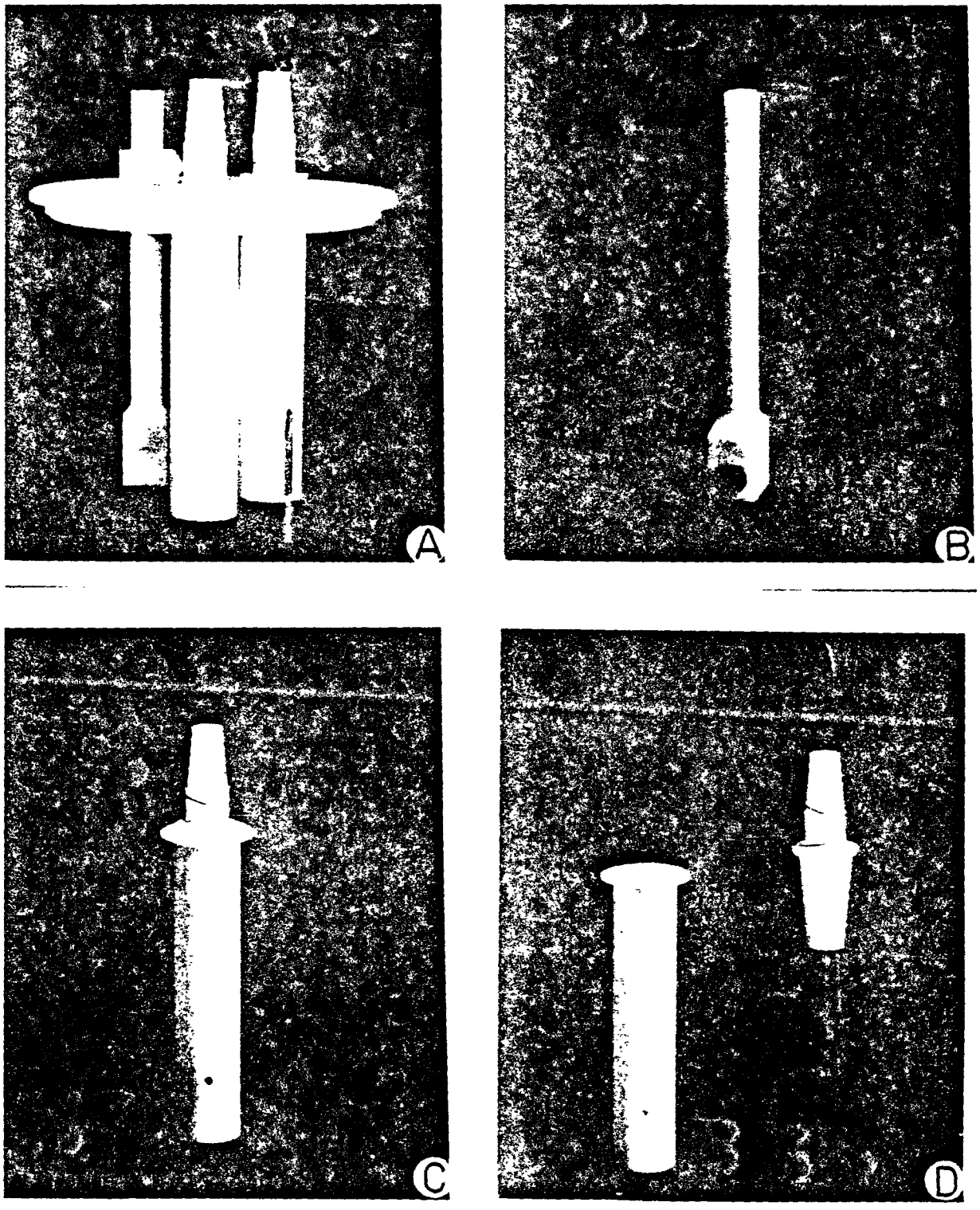

C REF. CELL

D REF. ELECTRODES

Figure 4: Photograph of cell assembly showing the various compartments and electrodes.

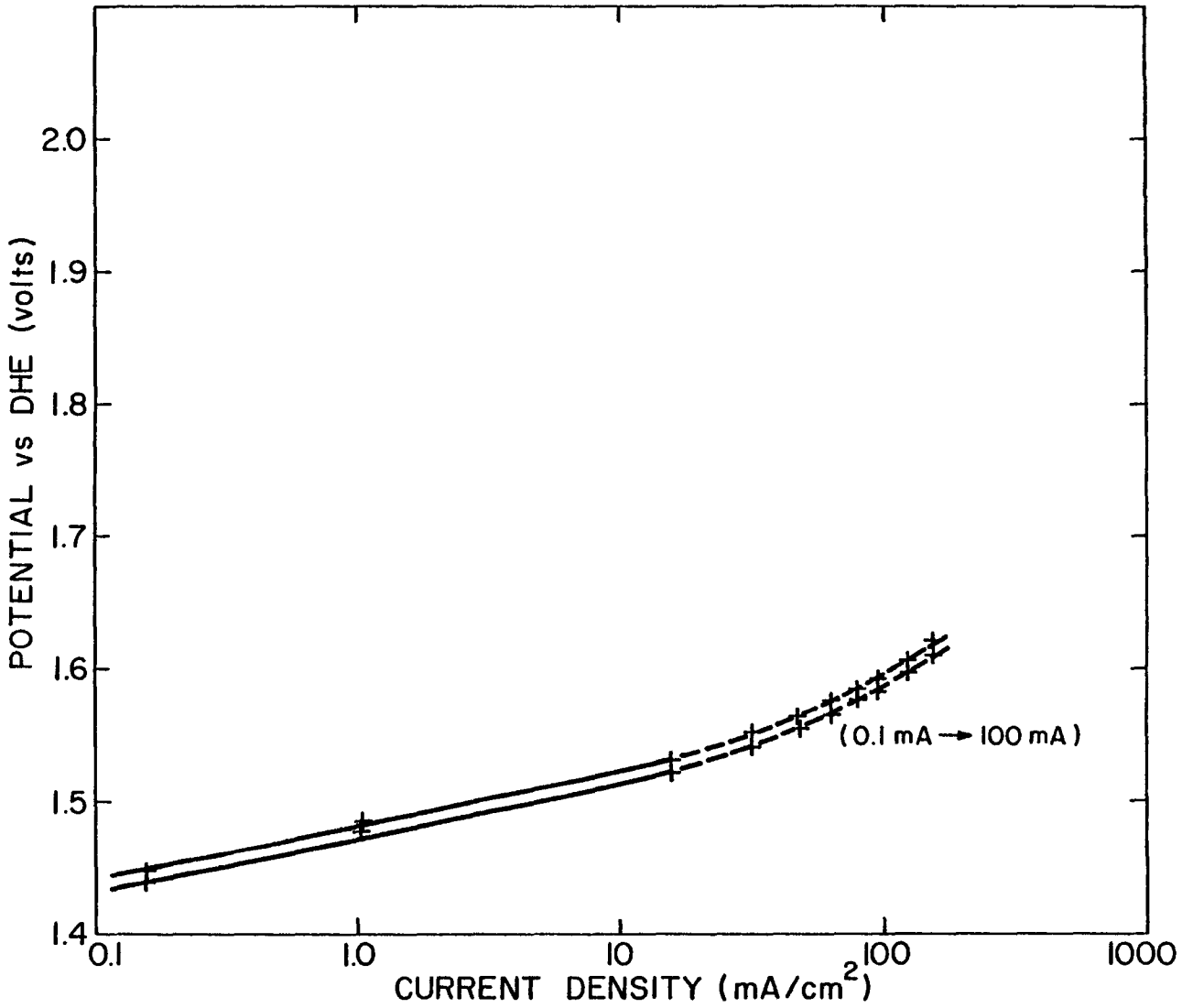

Figure 5: Current-potential curve obtained for the Ni electrode coated with Polymethana backing.

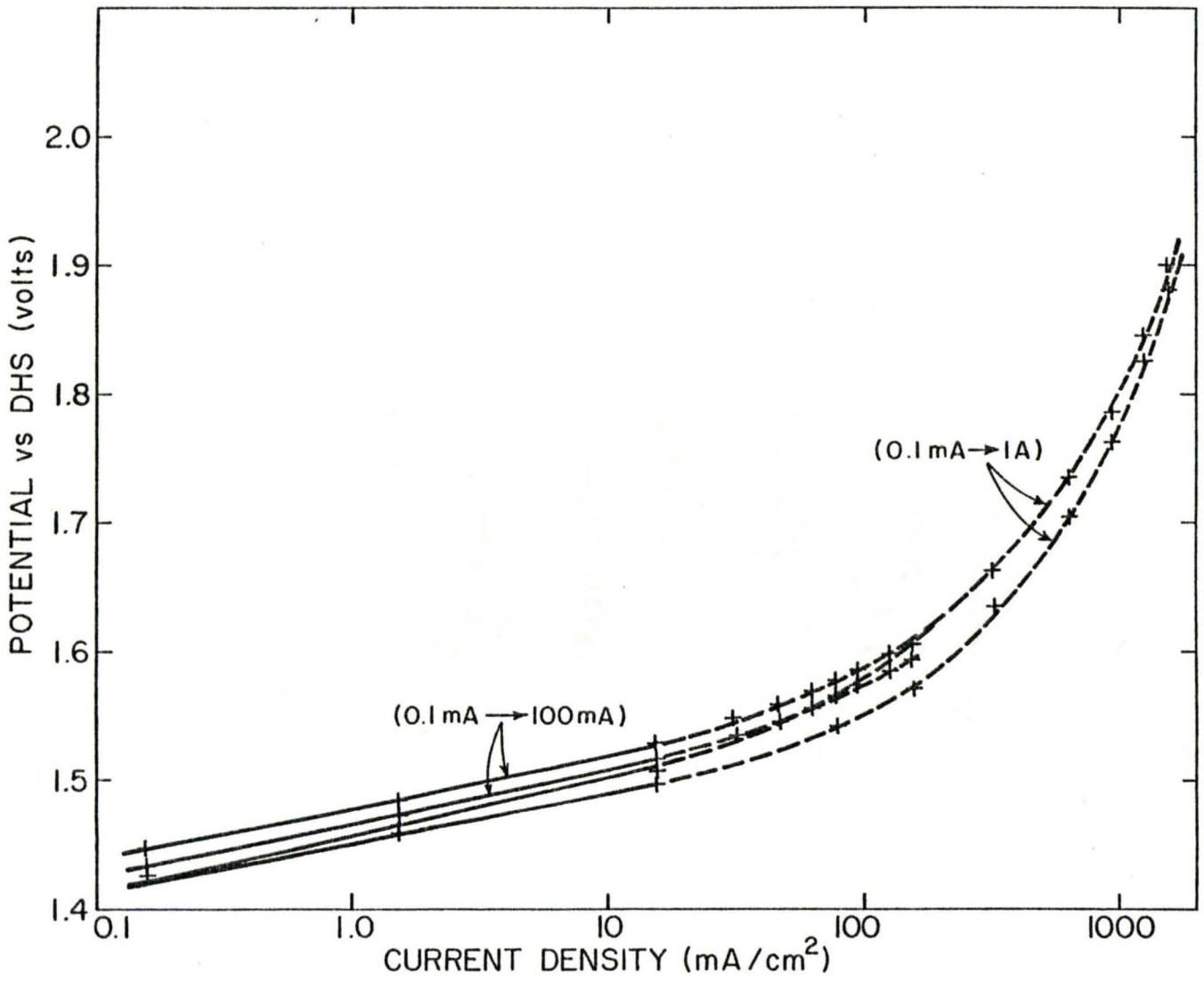

Figure 6: Current-potential relation for N_i with parafin wax backing.

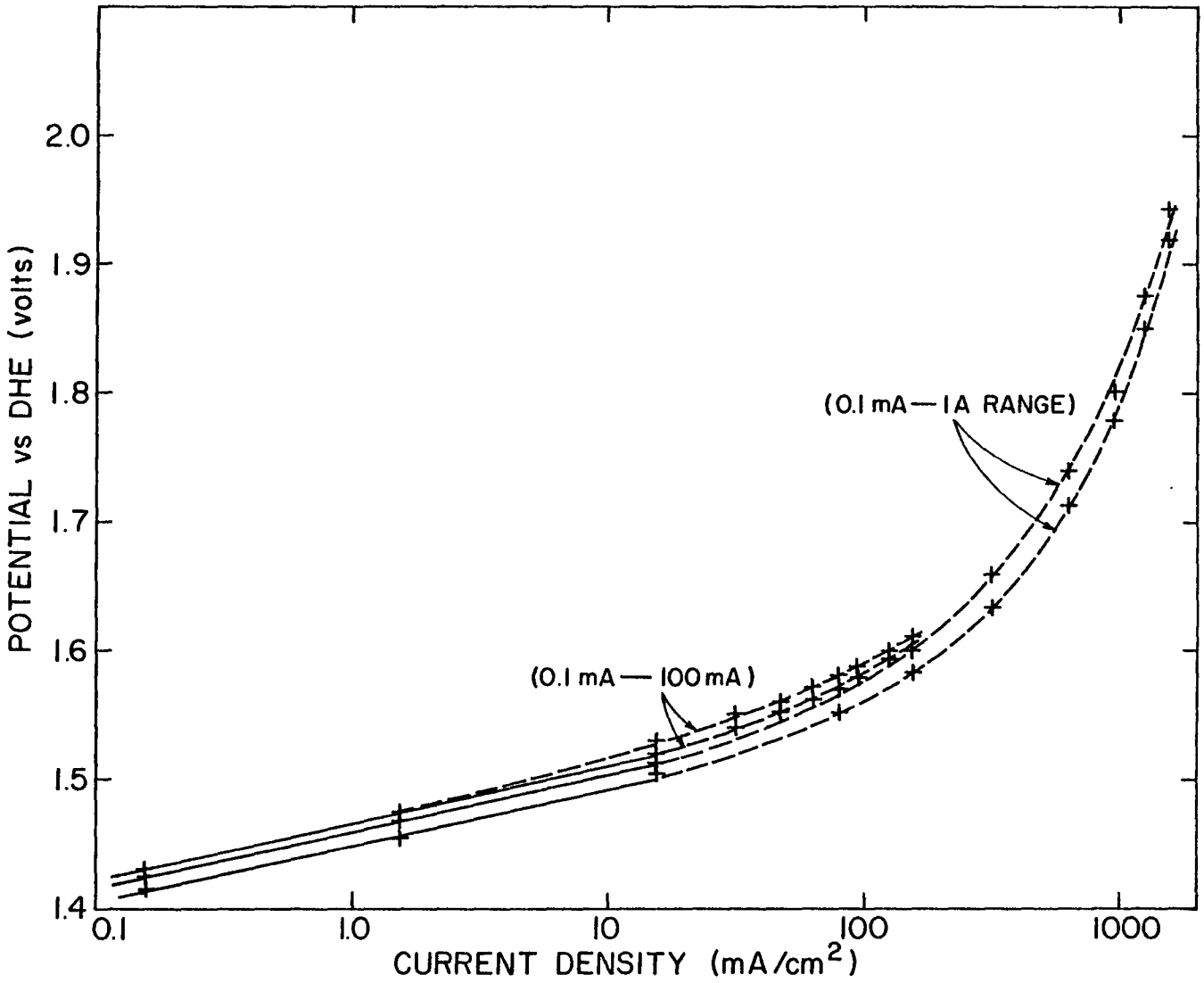

Figure 7: Current-potential curve for the Ni electrode coated with 5 minute epoxy backing.

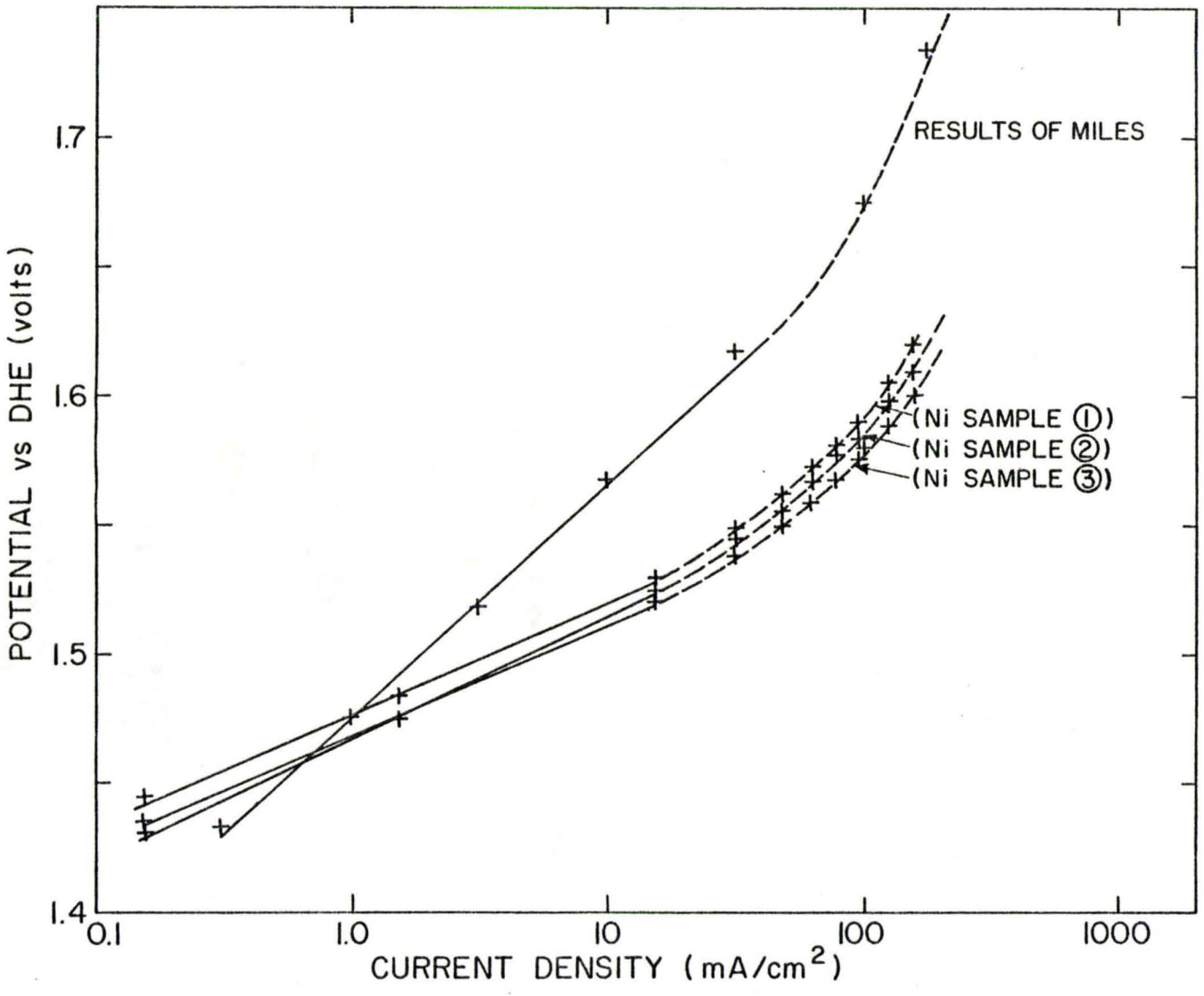

Figure 8: Oxygen evolution current-potentials on polished Ni electrodes compared to that of Miles[24].

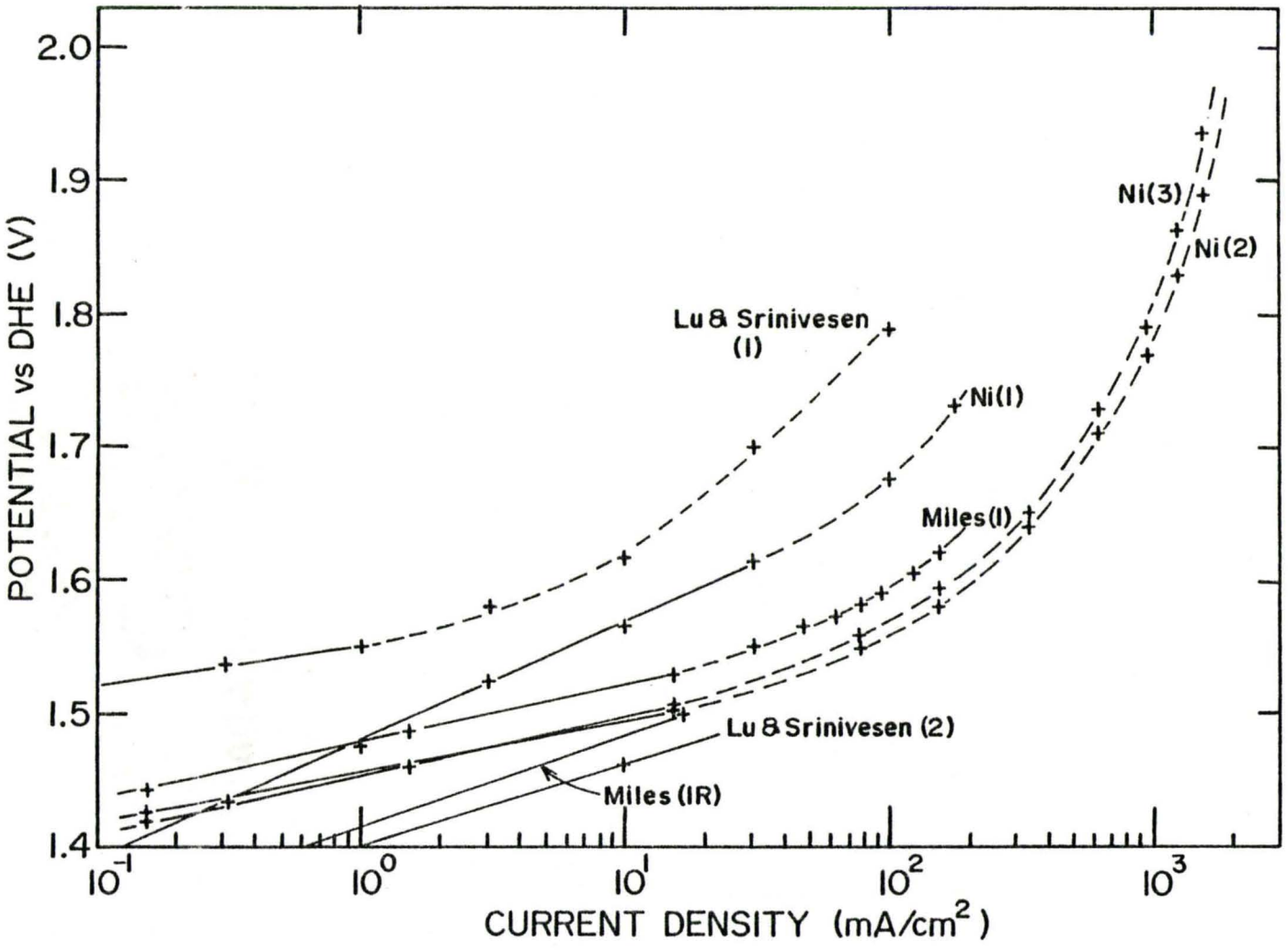

Figure 9: Current-potential relations obtained for polished Ni electrodes compared to that of Miles and Srinivasan.

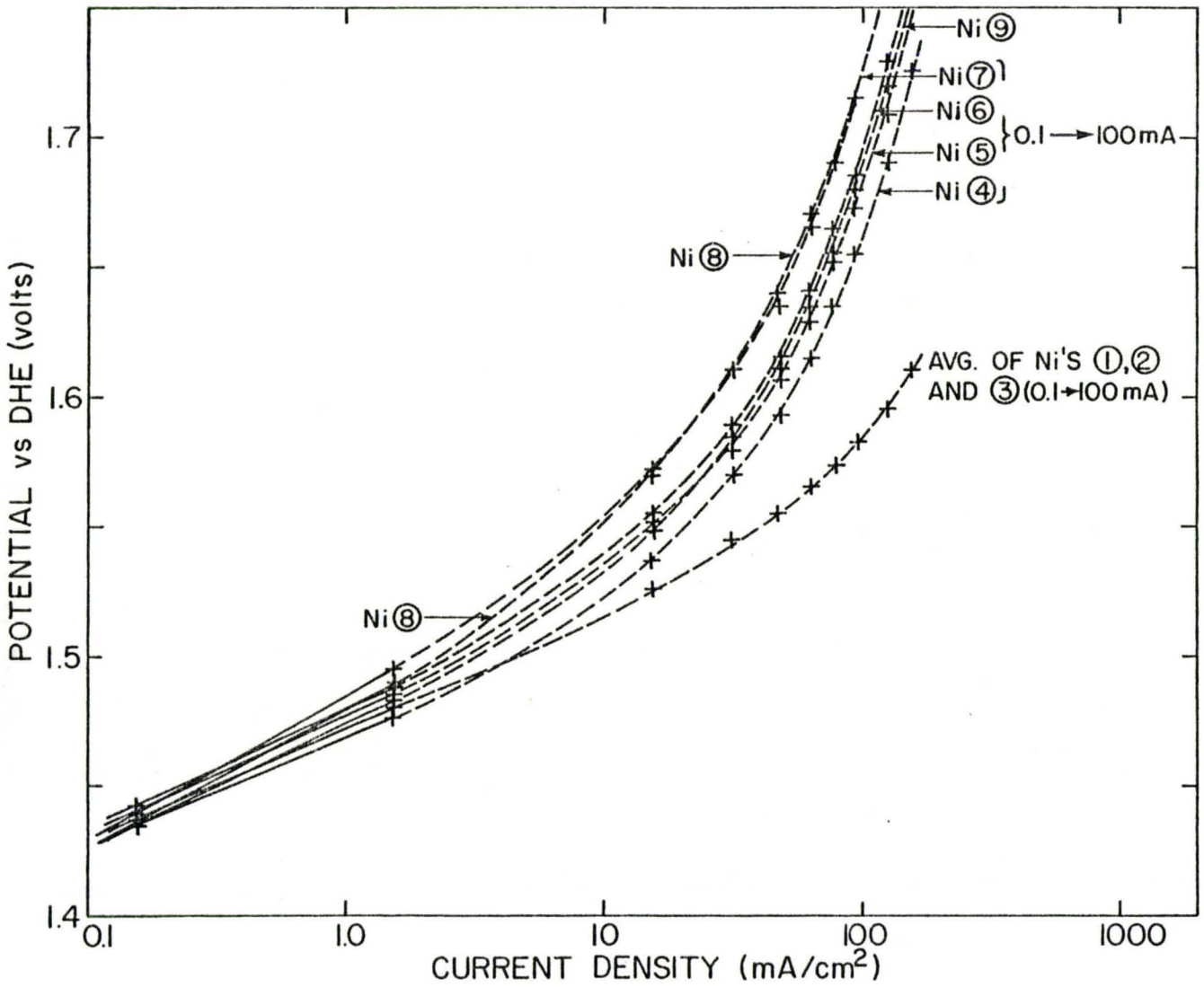

Figure 10: Current-potential relation for test electrodes with different Teflon holders (low current density).

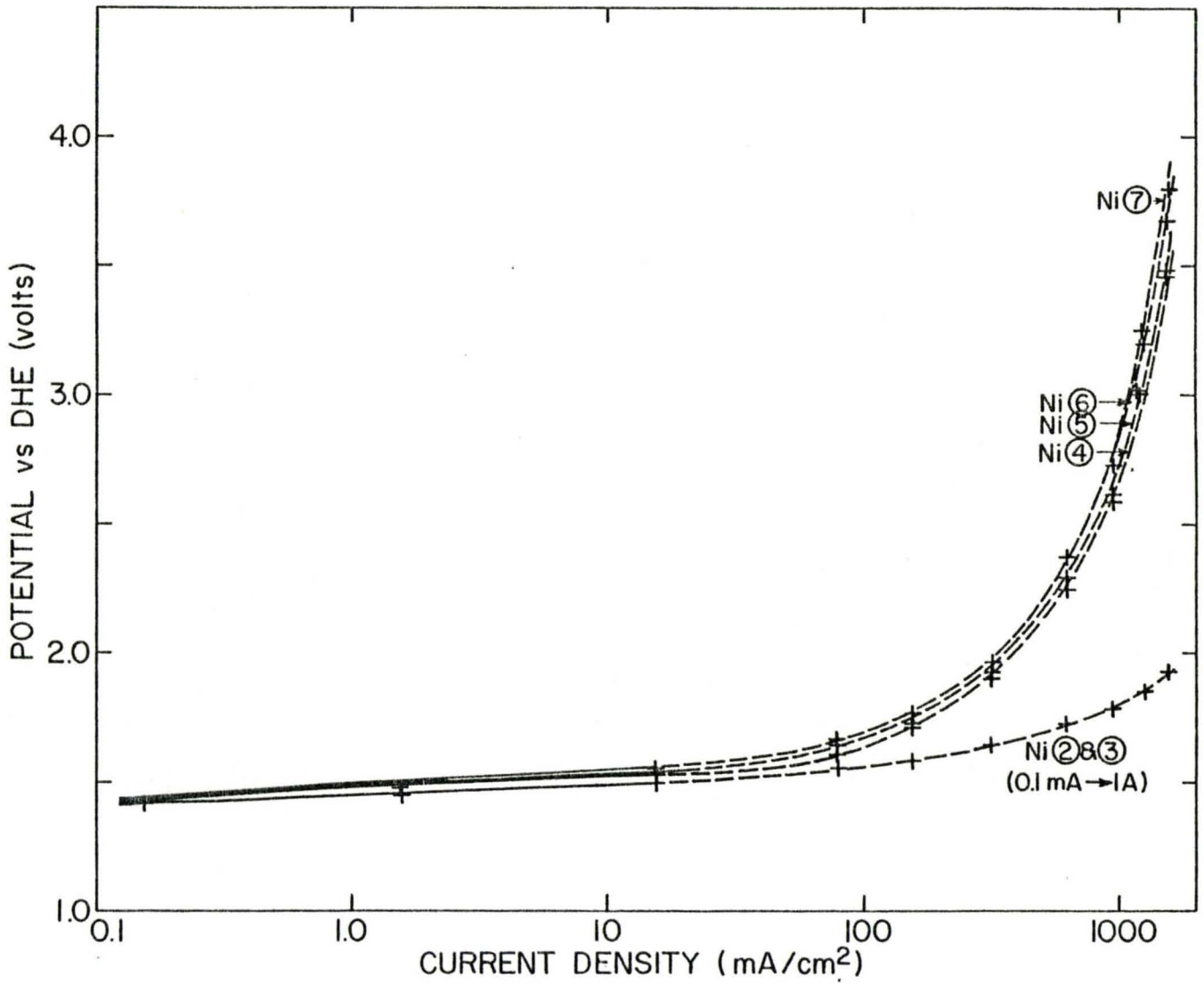

Figure 11: Oxygen evolution potential vs. log of current density for polished Ni electrodes using different teflon holders (high current density).

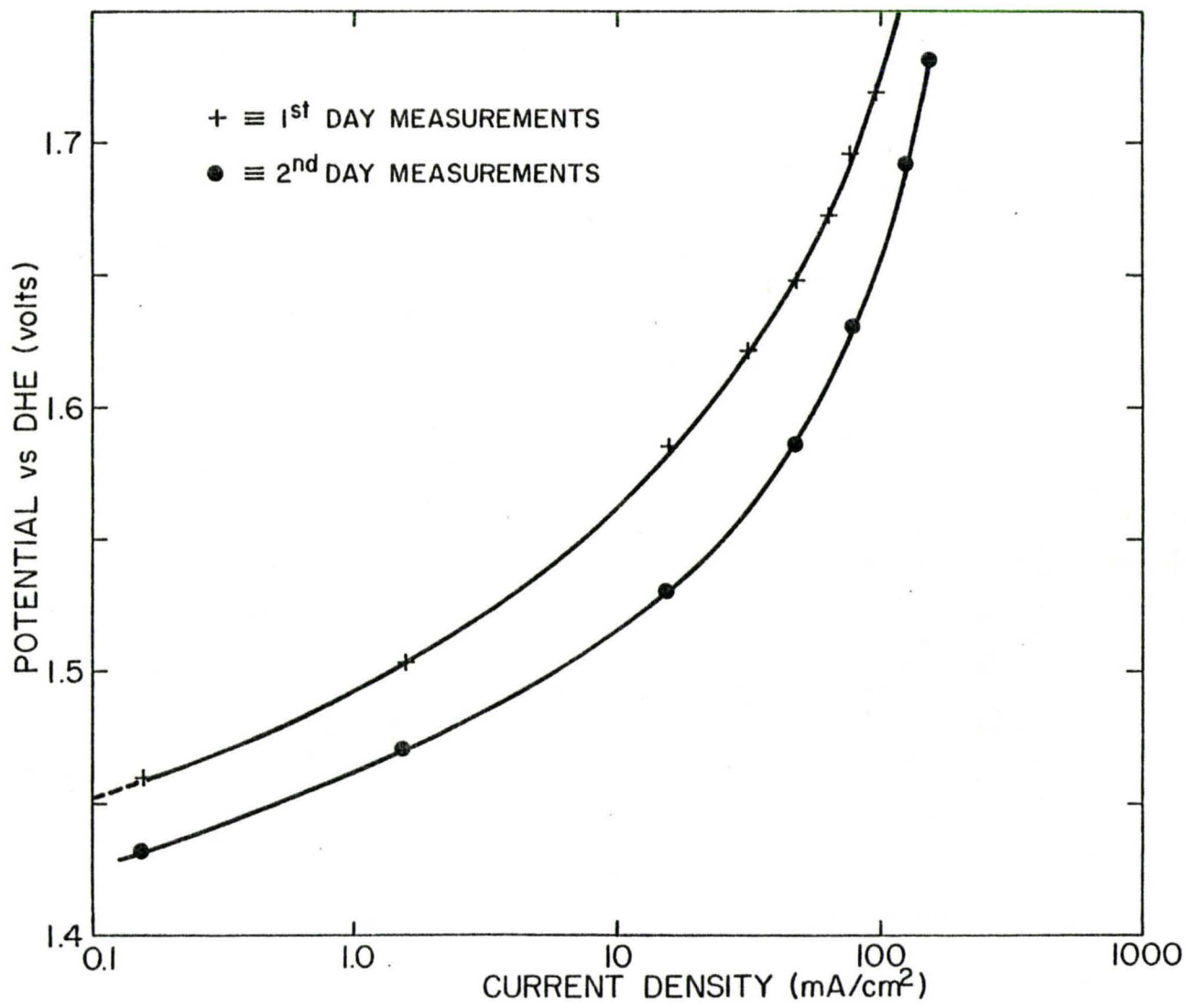

Figure 12: Oxygen evolution potential on NiO electrode vs. log of current density (low current density).

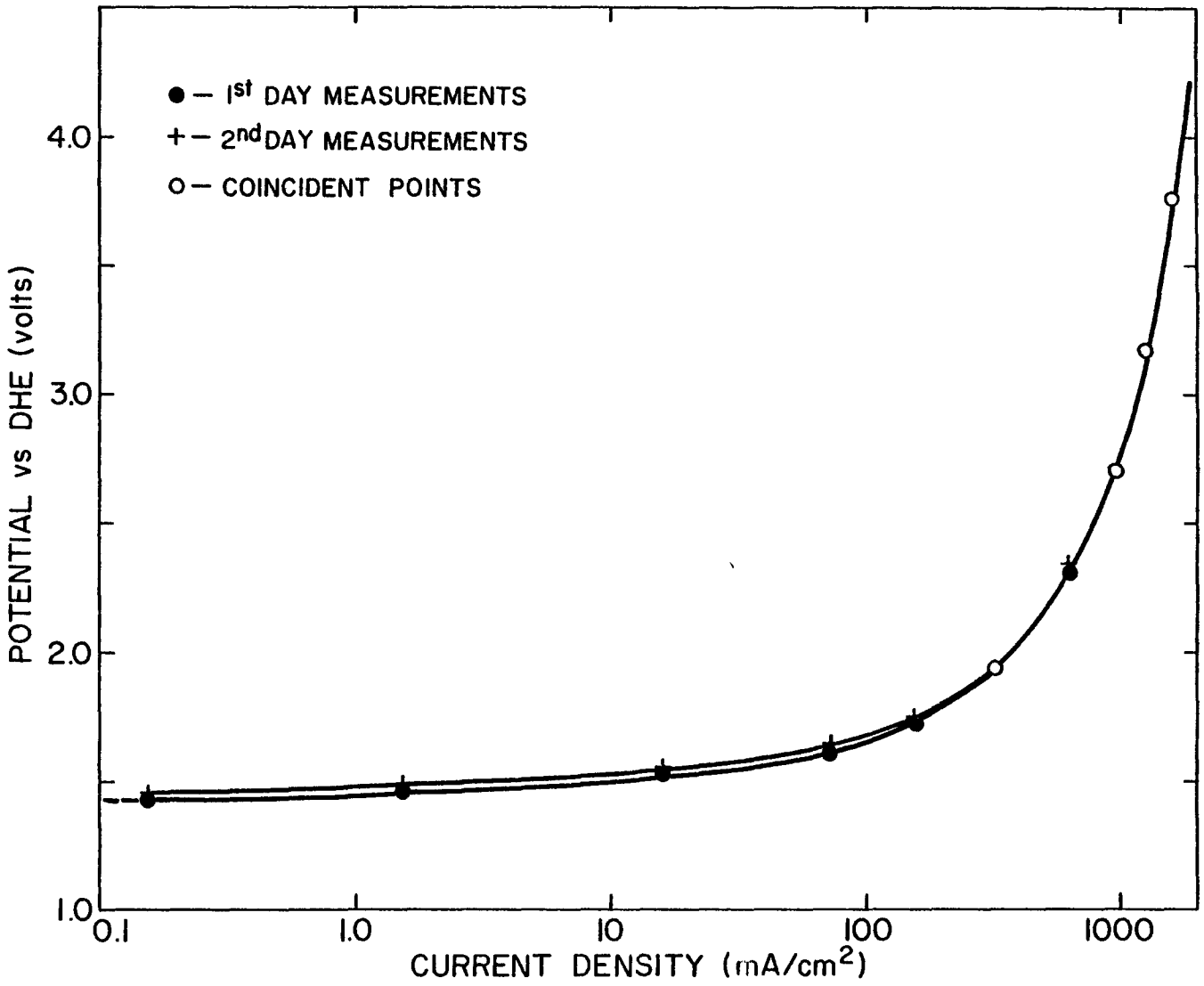

Figure 13: Oxygen evolution potential on NiO electrode vs. log of current density (high current density).

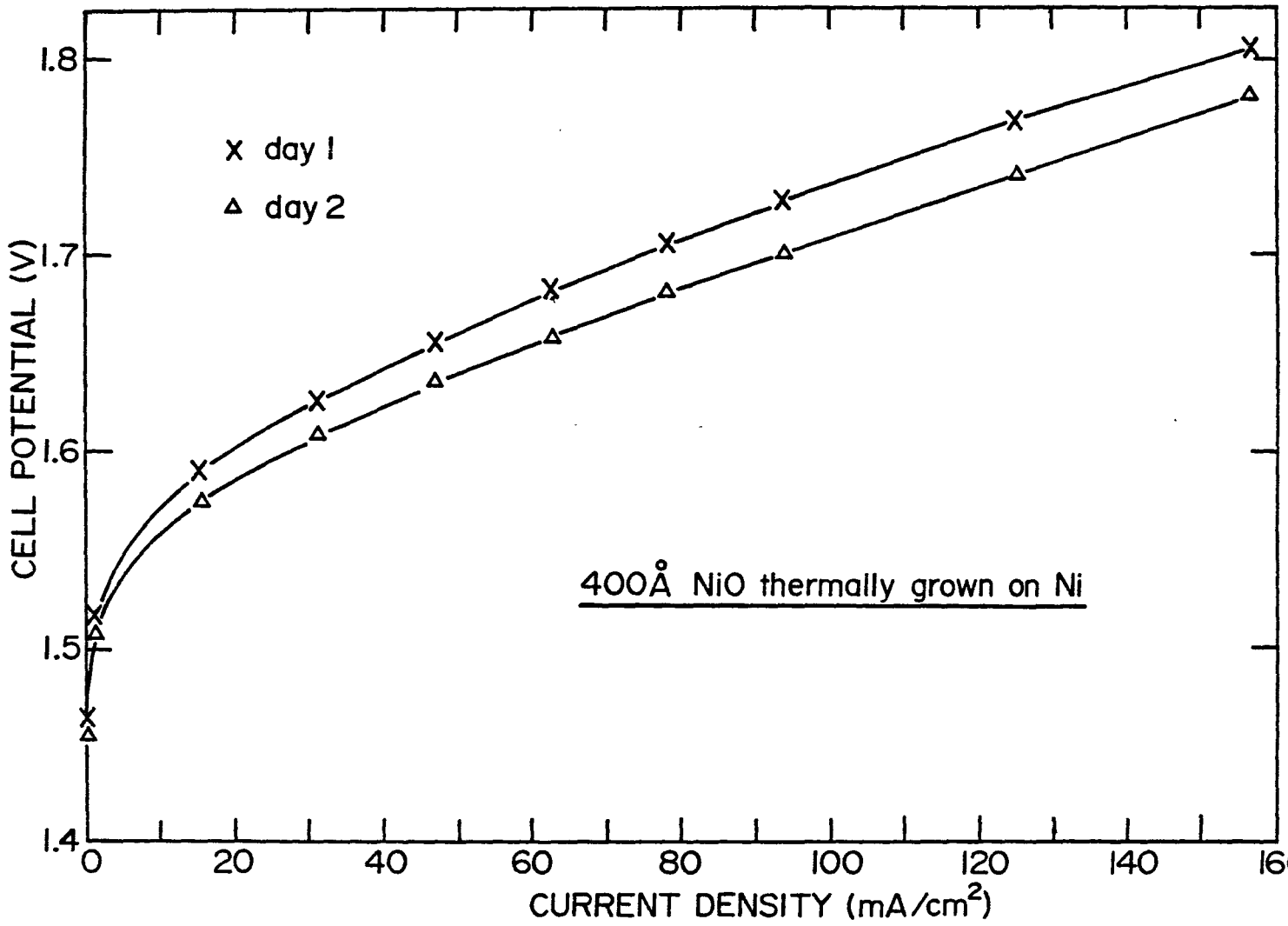

Figure 14(a): Oxygen evolution potential on 2nd NiO electrode vs. current density (low current density).

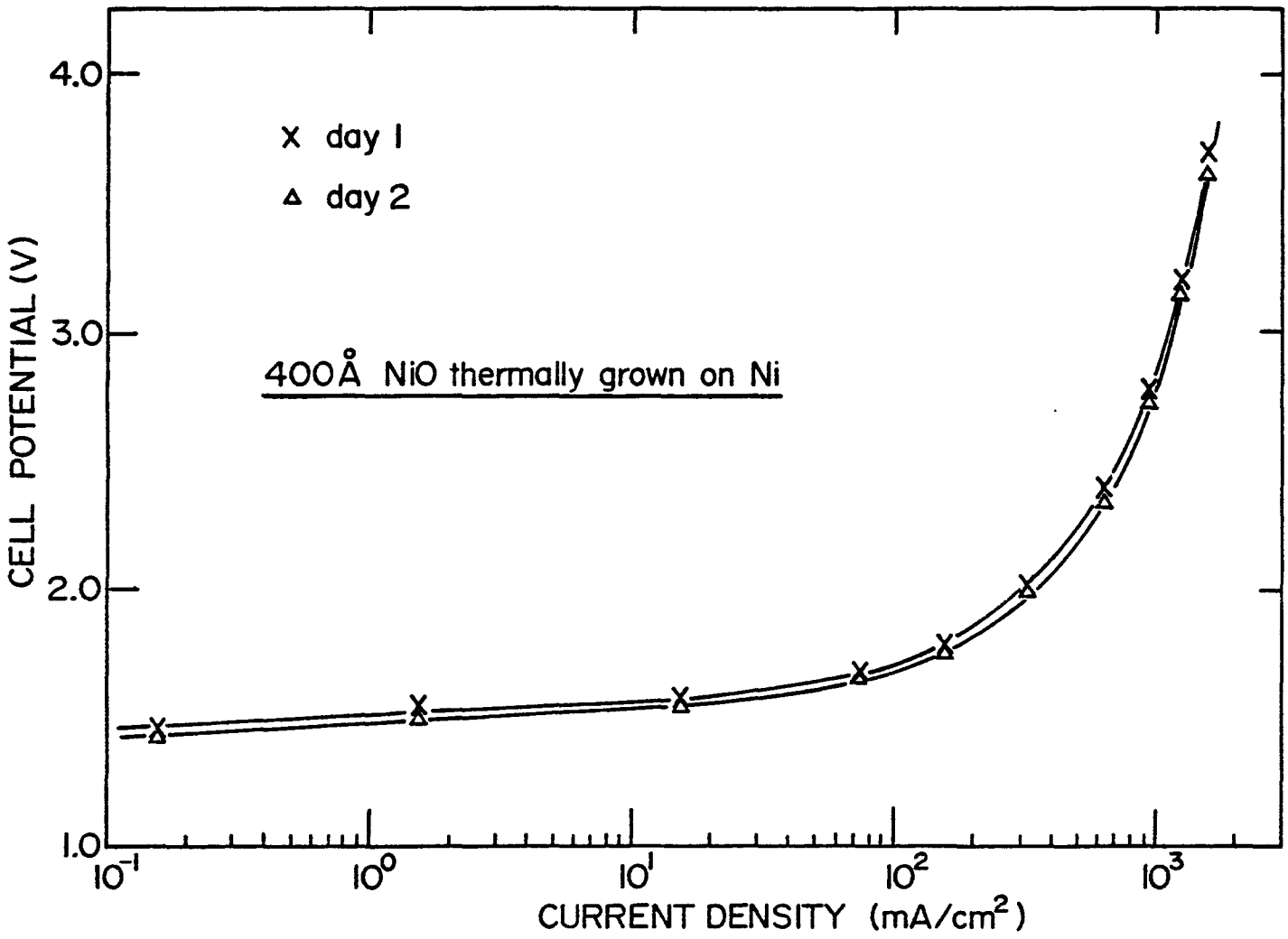

Figure 14(b): Oxygen evolution potential on 2nd NiO electrode vs. log of current density (high current density).

Ni(5)

Ni(6)

FIG 14(c) OPTICAL MICROGRAPH OF Ni ELECTRODES

Ni(5)

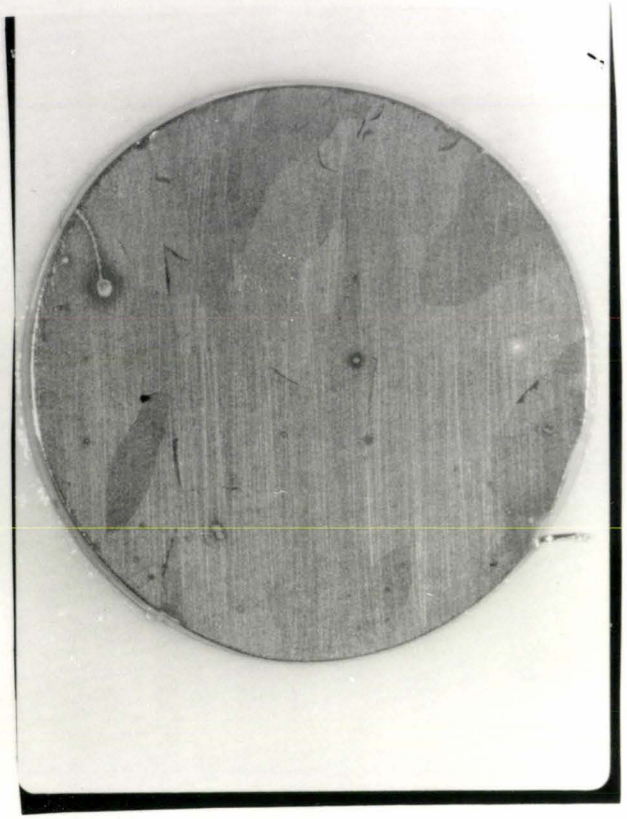

Ni(O)-Ni

FIG 14(c) OPTICAL MICROGRAPH OF ELECTRODES

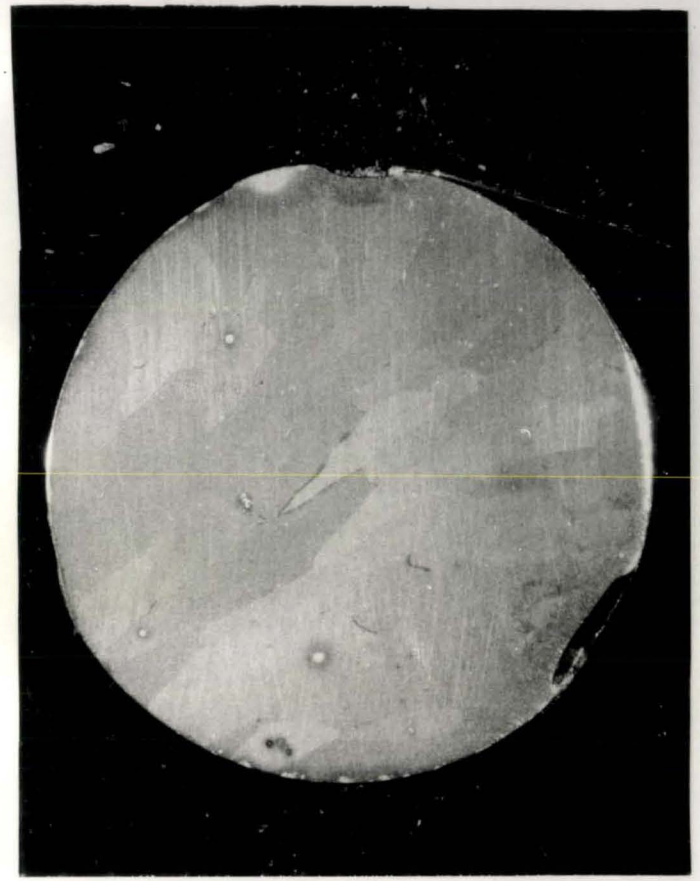

AS GROWN NiO

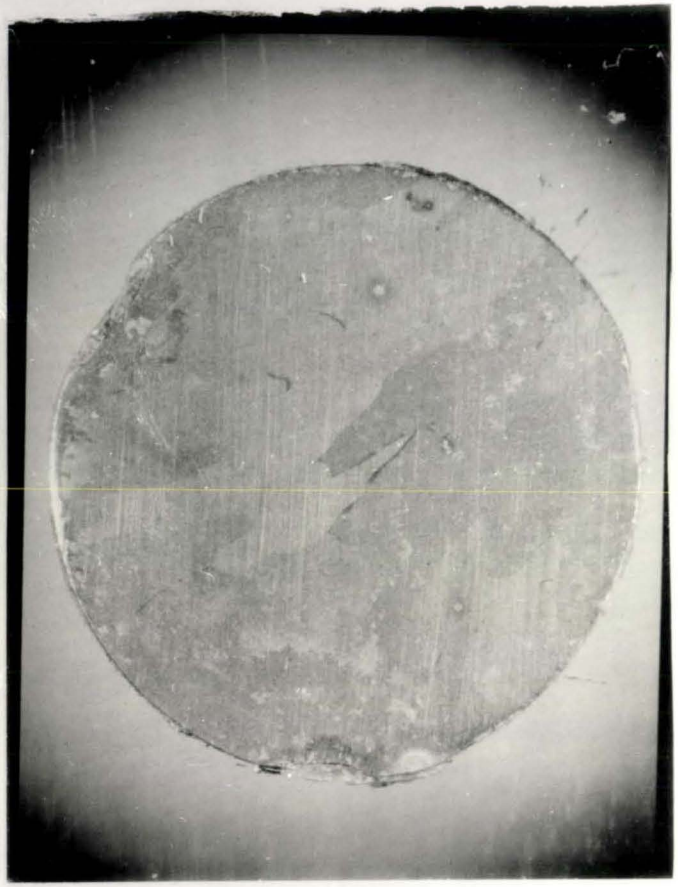

SAMPLE AFTER POLARIZATION

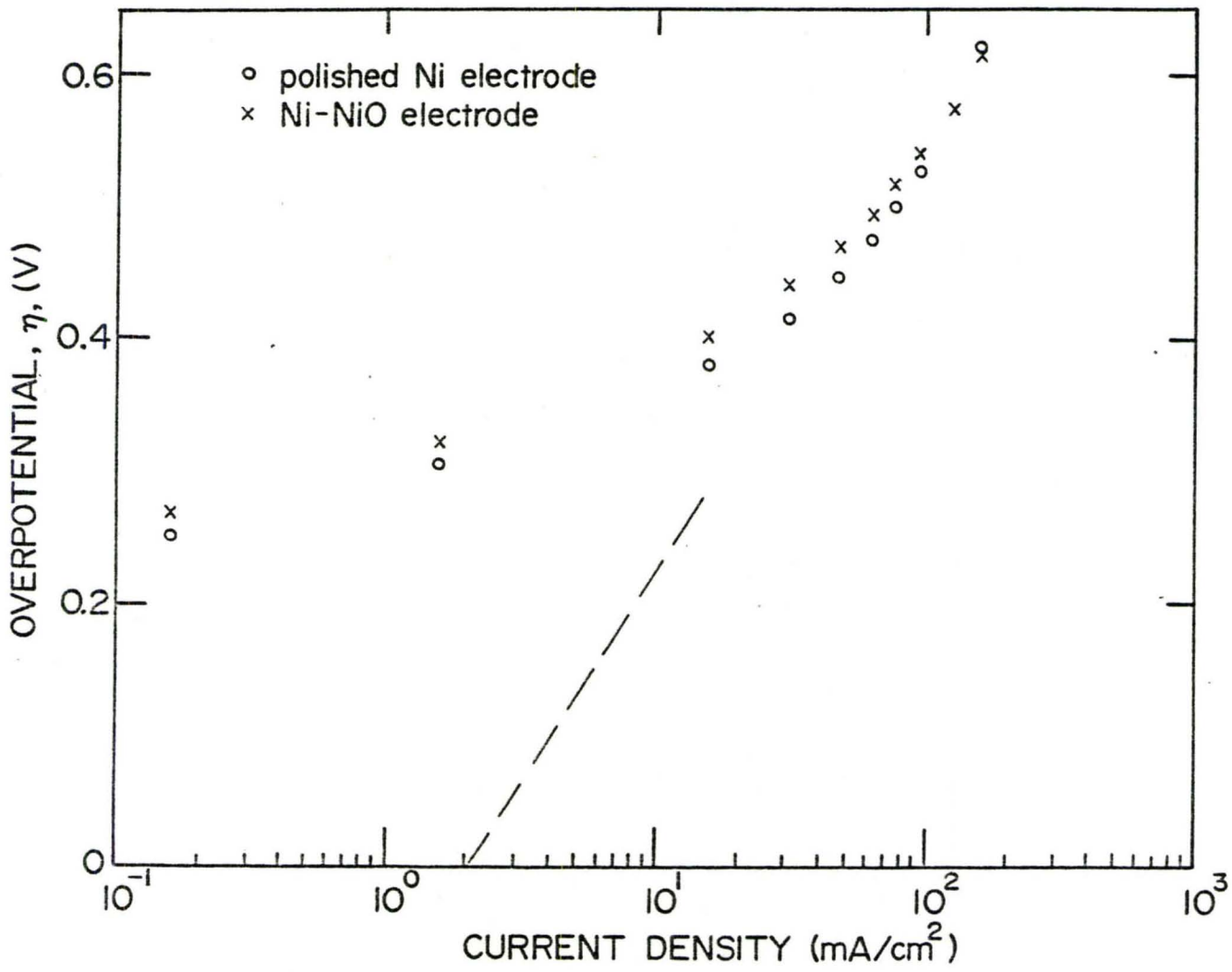

Figure 15: Oxygen overpotentials vs. log of current density (low current density).

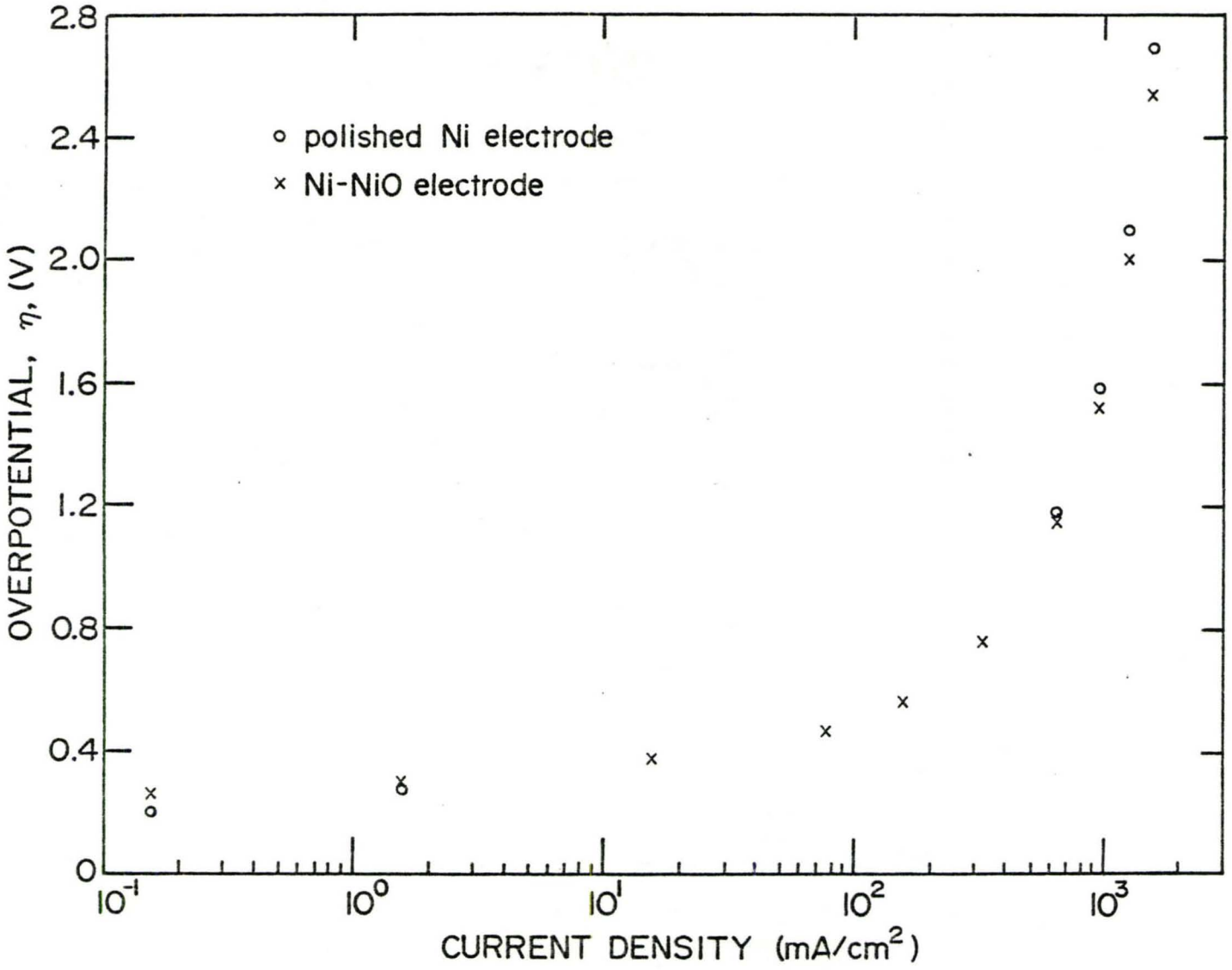

Figure 16: Oxygen overpotentials vs. log of current density (high current density).